For the degree of MSc (Med) in the Department of Immunology at the University of Cape Town

The Role of Endotoxin Receptors Toll-like Receptor 4 and Lipopolysaccharide-binding Protein in *Mycobacterium tuberculosis* Infection

By

Brian Abel

Under the supervision of Professor Bernard Ryffel

Acknowledgements:

Prof. Bernard Ryffel, for his generosity, patience and for supervising my thesis.

My mother and father, for supporting me during my studies, for their continual interest in my work, and for tolerating me always. For their unconditional love.

Nicole, for her love and support from afar.

Alex, for her love, understanding and for bearing with my procrastinations.

Muazzam (Teddy J), for his advice and assistance whenever needed.

Senate (Senaughty), for her moral support and caffeine-driven late-night session sharing.

Kamsellin (KC), for last-minute assistance, conversations and tandoori.

Najmeeyah (Naji), **Nasiema** (Nasi-goreng) and **Sumayah** (Candy), for assistance and the much-needed coffee-breaks together.

Lizette and Shireen, for assistance with IHC and maintaining the P3 unit.

Barbara, for her initial supervision and continued interest.

Wendy (Winderig), for her assistance with tissue-cutting, Zns and Hes.

Rob, for his proof-reading, corrections and encouragement.

Berenice (Berritjie), for her support, and company on the other side.

Prof. Frank Brombacher, for advice, and for the generous supply of antibodies.

Prof. Stan Ress, for moral support, encouragement and advice.

Mark, for his standardisation of ELISAs and organisation.

Noel and Hiram, for carrying out mouse orders, and for assistance where-ever needed in the animal house.

Durayah, for her assistance with all things bureaucratic and advice.

Connie, for her assistance and for supplying me with all sterile-ware.

The Role of Endotoxin Receptors LBP and TLR4 in *Mycobacterium tuberculosis Infection*

1 Introduction

1.1 The Immune System

In the course of evolution, multicellular organisms have developed immune mechanisms that render them inhospitable to invading microorganisms. These mechanisms are able to differentiate self from non-self, and to further identify the pathogen present in order to mount the most effective response. This comprises two distinct components: the innate immune system and the acquired immune system. The innate immune system functions immediately upon infection and requires no prior exposure to the pathogen. It is based primarily upon phagocytic cells, which engulf pathogens and subsequently elaborate cytokines and chemokines that orchestrate inflammation and prime the development of the acquired immune response. When a foreign invader eludes the mechanisms of the innate immune response, a more specific acquired immune response is elicited. Acquired immunity is mediated by B and T lymphocytes expressing unique receptors with remarkable antigen-specificity. These cells are clonally expanded upon engagement of their receptor by appropriate antigen. The nature of pathogen determines the types of stimuli generated by the innate immune response, and hence the appropriate polarisation of acquired immunity. This can develop in two directions: (i) a cellular response mediated by the T-helper 1 (T_H1) subset of $CD4^+$ cells and $CD8^+$ T cells which secrete pro-inflammatory cytokines to activate macrophages and enable intracellular killing, or (ii) a humoral response mediated by $CD4^+$ T_H2 cells which secrete anti-inflammatory cytokines to de-activate macrophages and promote the differentiation and expansion of B cells into antibody expressing plasma cells.

1.2 The Immune Response to *Mycobacterium tuberculosis*

Tuberculosis, caused by *Mycobacterium tuberculosis* (*M.tb*), is responsible for 1.5 million deaths per year worldwide and has reached epidemic proportions in southern Africa exacerbated by immunodeficiency secondary to HIV/AIDS infection. Phagocytes activated by T lymphocytes and cytokines (eg. IFNγ, TNFα and IL-12) usually control this infection in most people, but in 10% of infected subjects, re-activation of latent infection results in active tuberculosis (1). To develop a vaccine against this major killer, a better understanding of the protective immune response is required.

Tuberculosis is contracted by the inhalation of droplets containing bacilli into the airways and alveolar spaces in the lungs (2). Once the bacillus is deposited onto the pulmonary epithelial surface of the alveoli, it is usually engulfed by an alveolar macrophage, which transports the pathogen into the lung parenchyma and draining lymph nodes. Following phagocytosis by the host macrophage, *M.tb* resides in a phagosome in which it begins to replicate, and is able to survive by retarding phagolysosome formation (3). *M.tb*-derived proteins are shuttled through the endosomic pathway, degraded, and peptides thereof associate with MHC class II molecules. Peptide-MHC II complexes are subsequently exported to the cell surface and presented to antigen-specific $CD4^+$ T cells. The infected macrophage secretes a milieu of effector molecules, including cytokines and chemokines, which promote the recruitment of additional blood monocytes and neutrophils. Eventually, lymph node-derived $CD4^+$ T cells and natural killer (NK) cells traffic to the inflammatory foci. Macrophage-derived Interleukin-12 (IL-12) and appropriate antigenic priming results in the clonal expansion and differentiation of antigen-specific T_H1 $CD4^+$ T cells (4). These activated T cells and NK cells secrete interferon-gamma (IFN-γ) which activate tuberculostatic macrophages and augment antigen presentation by enhancing MHC II expression. Activated macrophages secrete tumour necrosis factor alpha (TNFα), which in synergy with IFNγ induces the release of mycobacteriocidal reactive nitrogen intermediates (RNI) including nitric oxide (NO) which has potent anti-microbial activity. TNFα has also been shown to enhance recruitment of cells by upregulating vascular adhesion molecule (5). Inability of the macrophage to fully eliminate the pathogen leads to the development of granuloma structures, which suppress the replication of the bacilli (6). These structures comprise a central core of activated macrophages, epithelioid cells and multinucleated giant cells surrounded by $CD4^+$ T cells. *M.tb*-derived proteins have also been shown to access the MHC I pathway as a consequence of (i) escape

from the phagosome into the cytoplasm (7) or (ii) translocation of mycobacterial proteins into the cytoplasm during persistent replication. This mechanism results in lysis of the infected macrophages by MHC I-restricted $CD8^+$ cytotoxic T cells, release of the bacilli and subsequent phagocytosis by newly immigrated and freshly activated macrophages (8).

1.3 Pattern Recognition of Pathogens by Antigen-Presenting Cells

Once a pathogen has succeeded in penetrating the physiologic barriers of the host, it is essential that the innate immune response be rapidly induced and focused in instructing acquired immunity. It is equally important, however, that the immune response is induced upon exposure to microbial-derived antigens and not upon the recognition of self-antigens, or innocuous, non-self antigens (9). Induction of the acquired immune response depends on the expression of co-stimulatory molecules and cytokines by antigen presenting cells (APCs). The mechanisms that control the initial induction of these signals are not well characterised. It has been suggested that cells of the innate immune system detect the presence of an infection by means of evolutionarily selected receptors that recognise highly conserved molecular patterns shared by broad classes of pathogens (10). These receptors have been termed Pattern recognition Receptors' (PRRs) and the molecular signatures they recognise 'Pathogen Associated Molecular Patterns' (PAMPs) (refer to fig. 1.1 and fig. 1.2). PRRs appear to be the elusive link between the detection of an infection and the instruction of the subsequent acquired immune response.

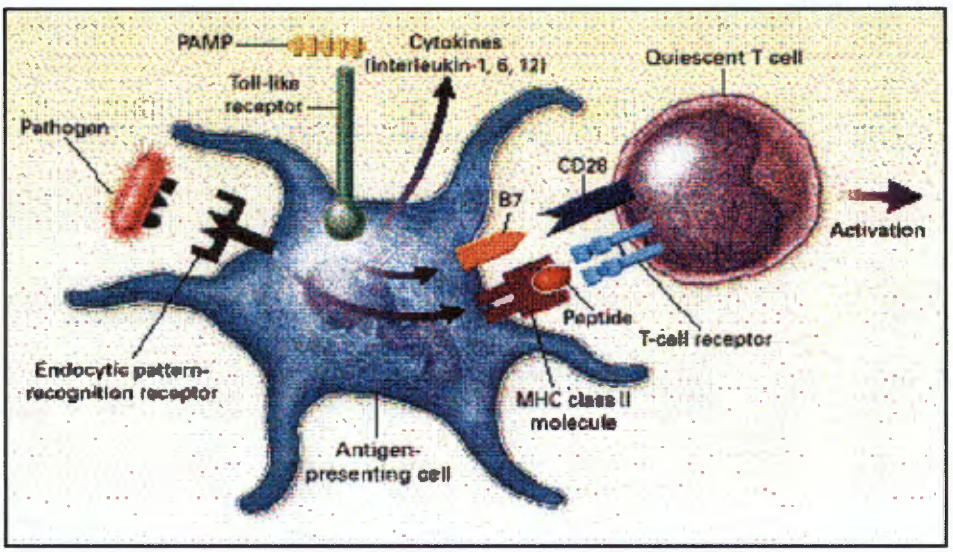

Fig. 1.1: Detection of a pathogen by its molecular signature (PAMP), initiation of an innate immune response, and instruction of the acquired immune response. (From Medzhitov *et al.* 2000)

1.4 Drosophila Toll, mammalian Toll-like receptors and Innate Immunity

The Drosophila protein toll was first described as mediating a role in the development of dorsoventral polarity during embryogenesis (11). Subsequently, infectious studies with adult Drosophila toll mutants (using flies expressing thermo-sensitive alleles of toll) revealed an essential role in the host antifungal response (12). Upon recognition of fungal invaders, a proteolytic cascade is activated, which terminates with the cleavage of the endogenous ligand pro-spatzle to its active form spatzle. Spatzle binds to the Drosophila toll (dToll) protein, which triggers an intracellular cascade terminating with a NFκB-like transcription factor termed dorsal. Dorsal binds upstream of the antifungal peptide gene drosomycin, activating its transcription and promoting host survival. The recognition of sequence similarity between cytoplasmic portions of dToll and that of signalling IL-1R components (termed the toll-IL-1R module or TIR module) indicated that there was evolutionary conservation of pathways implicated in innate immunity. The first member of the mammalian toll family (named toll-like receptors or TLR) to be identified and cloned was human Toll (hToll) based on its homology to dToll (13). This lead to intensive investigation in the field of mammalian TLRs, and to date almost ten TLRs have been cloned in mouse and man. The murine TLR4 involved in the recognition of the Gram-negative product LPS, and TLR2, implicated in the recognition of Gram-positive products, have both been observed *in-vitro* to be involved in response to *M.tb*. This has initiated exciting studies, which will hopefully further our understanding of the development of protective immunity to *M.tb*.

In the context of this thesis, I investigated the role of the endotoxin receptors LBP and TLR4 in the host resistance of mice to *M.tb*., therefore this review is focused on these PRRs.

Endotoxin from Gram-negative bacteria binds to an acute phase protein, LPS binding protein (LBP), which has properties of a PRR (14) and enhances LPS binding to the soluble and membrane CD14 receptor (15). The LPS complex associates with the recently discovered TLR4, which is the signalling receptor, implicated in the activation of a kinase cascade. This cascade in turn activates the transcription factor NF-κB leading to transcription of pro-inflammatory genes. Recently, a single amino acid mutation of TLR4 in C3H/HeJ mice was proposed to be responsible for their LPS resistance (16,17). This implicates TLR4 in LPS signal transduction. Mycobacterial cell wall components were shown to bind to the LPS receptor CD14 (18,19,20), however the role of this interaction in the induction of APCs and

host resistance to *M.tb* is not established. Utilising gene deficient mice for LBP (21), CD14 (22), and TLR4 (23), one can determine whether the LBP/CD14/TLR4 mediated uptake and activation is critical for defence against *M.tb* infection and the induction of protective immunity.

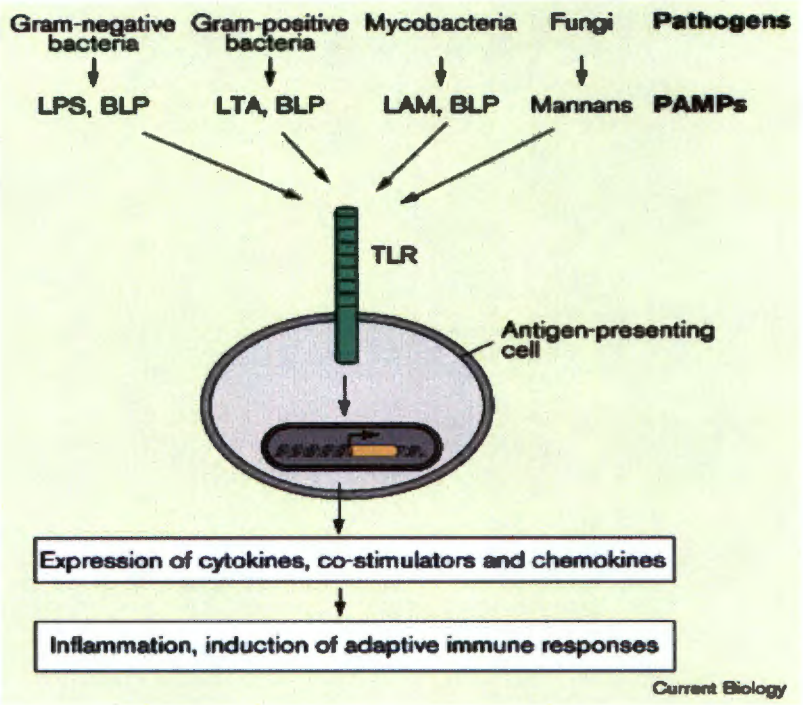

Fig. 1.2: Recognition of these PAMPs by TLRs on APCs activates the expression of various factors that lead to inflammatory responses and the induction of acquired immunity. LPS = lipopolysaccharide, BLP = bacterial lipoproteins, LTA = lipoteichoic acid, LAM = lipoarabinomannan (From Medzhitov et al. 1999).

1.5 Molecules investigated *in vivo* in *Mycobacterium tuberculosis* infection

1.5.1 Toll-like Receptor 4 (TLR4)

It has been well documented that the inflammatory response to LPS is initiated at the surface of myeloid cells by the binding of LPS to the glycosylphosphatidlyinositol (GPI)-linked protein CD14 (24). Since GPI-linked proteins cannot tranduce their own signals, another protein was speculated to be responsible for this function. Investigation of LPS responsiveness lead to the discovery that the C3H/HeJ mice had acquired a mutant phenotype through spontaneous mutations, which occurred during 1960 and 1968. (25) Genetic analysis established that this phenotype is under the control of a single locus named *Lps* on chromosome 4, existing in two allelic forms, Lps^n (responsive) and Lps^d (hyporesponsive) (26). C3H/HeJ mice were found to have a point mutation within the coding region of the Tlr4 gene (16,17). A base transversion (C→A) in the third exon of the gene caused the substitution

of a histidine for an evolutionarily conserved proline at residue 712. The C3H/HeJ strain exhibits a remarkable tolerance to otherwise lethal doses of LPS, and several cell types, namely macrophages, B cells and fibroblasts are hyporesponsive to LPS in vitro. TLR4 is thus implicated as the early and essential part of the signal transduction machinery linking LPS with gene expression. The consequence of this mutation is that these mice are extremely susceptible to Gram-negative bacteria and succumb to an overwhelming infection (27). The role of TLR4 in sensing the presence of Gram-negative bacteria and triggering a lifesaving response is undisputed. In addition, TLR2- and TLR4-deficient mice confirm a critical role of TLR4 in endotoxin signalling (23) and demonstrate that TLR2, but not TLR4 is required for signalling by Gram-positive bacteria (28). *in vitro* experiments with Chinese Hamster Ovary (CHO) cells expressing human TLR2 or TLR4 indicated that they mediate responses to components of *M.tb* and may be important in instructing the subsequent acquired immune response (29). These findings implicate both TLR2 and TLR4 in the recognition of *M.tb*-derived PAMPs.

1.5.2 Lipopolysaccharide Binding Protein (LBP)

LBP is synthesised in hepatocytes as a single polypeptide and released into the blood as a 60 kDa glycoprotein (30). The synthesis of LBP is under the control of cytokines and steroid hormones, and it behaves as an acute phase protein (31). LBP catalyses the removal of LPS monomers from aggregates or bacterial membranes (refer to fig. 1.3) and transfers them to CD14, thereby enhancing the sensitivity of cells to LPS (32). LBP mutants were generated by disruption of the murine LBP gene locus by targeted homologous recombination in embryonic stem (ES) cells (21). Serum from animals homozygous for the mutation had no measurable LBP, and were found to be hyporesponsive to the co-administration of D-galactosamine and LPS intra-peritoneally. As seen with the C3H/HeJ mice, the inability to respond to LPS renders the LBP mutants highly susceptible to infection with Gram-negative bacteria such as *Salmonella typhi* (21). Experiments with human microglia indicated that *M.tb* uptake was mediated by CD14, and that the addition of LBP enhanced this process (33). Evidence that TLR4 is involved in both the recognition of Gram-negative bacteria and *M.tb* might indicate that PAMPs expressed on these organisms have similar structural patterns enabling the engagement of the same PRR. However, it was recently demonstrated that TLRs may be involved in the recognition of chemically unrelated PAMPs (28), adding another level of complexity to TLR biology. Since TLR4 is involved in the recognition of both endotoxin and

M.tb PAMP(s), we hypothesised that LBP may also mediate a role in the recognition and transfer of these PAMP(s) during a *M.tb* infection.

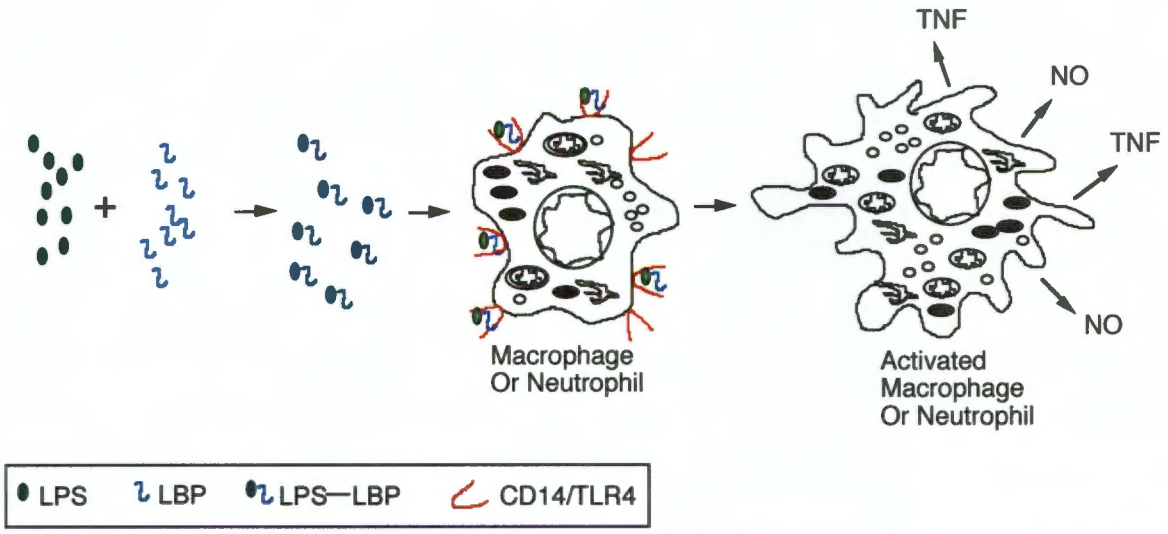

Fig. 1.3: Mechanism of LPS stimulation of CD14-expressing cells. Signal transduction is initiated by TLR4 and results in the potent transcription of pro-inflammatory genes.

1.6 Additional molecules measured during the *M.tuberculosis* infection

1.6.1 Interferon gamma (IFNγ)

IFNγ is a cytokine which plays a major role in the immune response to *M.tb.* Secreted mainly by Th1 CD4 cells and NK cells, it strongly primes for the development of the Th1 subset of cytokines, and serves as a potent activating stimulus for macrophages. IFNγ elicits bacteriacidal mechanisms including ROI, RNI, lysosymes and defensins (34). Mice genetically deficient for IFNγ display dramatically impaired production of antimicrobial products and reduced surface expression of MHC II molecules on macrophages. IFNγ-deficient mice succumb to a sublethal dose of the intracellular pathogen *Mycobacterium bovis* demonstrating the essential role mediated by this cytokine during mycobacterial infections (35).

1.6.2 Interleukin 12 (IL-12)

IL-12 is a pro-inflammatory cytokine produced by phagocytic cells, B cells and other antigen-presenting cells. It mediates a critical role in bridging the innate and acquired immune response by inducing IFNγ production of T- and NK cells, and it promotes the development

of the T_H1 subset of T cells (4). IL-12 is a heterodimeric protein (IL-12p75) comprised of two disulfide-linked subunits designated p35 and p40, which are encoded by unrelated genes (36). Both subunits can be induced by IFNγ (37). The secretion of IL-12p35 is the limiting factor for biologically active IL-12, and homodimers of the IL-12p40 subunits can serve as functional antagonists (4). Mice deficient for IL-12p40 displayed dramatically reduced protective immunity to *M.tb*, and succumb to infection (38).

1.6.3 Tumour necrosis factor alpha (TNFα)

TNFα is a cytokine, which is a potent mediator of inflammatory reactions and tissue damage. It is involved in the induction of fever symptoms, the acute phase response and enhancement of vascular permeability (5). An essential role for TNFα in mediating protection against mycobacterial infections has been demonstrated with TNFα-deficient mice, which succumb to infection. These mice have impaired development of granulomata (39,40) which suggests an essential role for TNFα in the development of these structures.

1.6.4 Monocyte chemoattractant protein 1 (MCP-1)

MCP-1 is a CC chemokine that attracts monocytes, memory T cells, and NK cells (41). Elevated levels of chemokines, including MCP-1 has been observed in bronchoalveolar lavage fluid of tuberculosis patients, suggesting an important role in the recruitment of inflammatory cells during infection (42).

1.6.5 Nitric oxide (NO)

NO is a potent RNI induced synergistically by IFNγ and TNFα. (43). NO and L-citrulline are generated by the metabolism of L-arginine, a reaction catalysed by the enzyme inducible nitric oxide synthase (iNOS). NO is a potent antimicrobial agent, which has been demonstrated to be essential for protection against mycobacterial infections. Mice deficient for the enzyme iNOS2 succumb readily to infection with mycobacteria (44).

1.7 Objectives

The aim of this study was to investigate the role of PRRs, namely TLR4 and LBP *in vivo* in the development of an immune response to a *Mycobacterium tuberculosis* infection. Mice with null mutations of the endotoxin receptors LBP and TLR4 were compared with wild-type mice (PRRs intact) in the context of an aerosol *M.tb* infection.

The following questions were posed:
Are the PRR-disrupted animals more susceptible to M.tuberculosis infection?
What role do these PRRs play in inflammatory processes and in the development of granuloma?
What role do the PRRs play in driving cytokine and chemokine response?

Specifically, the following mice were infected aerogenically with *M.tb* H37Rv to further investigate their roles *in vivo* in mounting an effective immune response:
C3H/HeN and C3H/HeJ (TLR4 mutant)
LBP+/+ and LBP-/-

2. Materials and Methods

2.1 Mouse Strains

Mice were bred and maintained under specific pathogen free (SPF) conditions in the animal unit at the University of Cape Town, South Africa. The animals were housed in filter-top cages and supplied with sterile water and food *ad libitum*.

Table 1: Mouse strains used in this study

Strain	WT background	Reference
C3H/HeJ	C3H/HeN	Charles Rivers Lab.
LBP -/- BALB/c x 129 SV	BALB/c +/+	Jack *et al (21)*

2.1.1 Genotyping of Gene-deficient Mice

The polymerase chain reaction (PCR) was performed routinely to confirm the genotype of all gene-deficient mice used in experiments. This method entails the amplification of DNA fragments, which have a known disruption.

2.1.2 Phenotyping of TLR4 mutants C3H/HeJ

The natural mutant C3H/HeJ, which has a single point mutation, was phenotyped by its hyporesponsiveness to lipopolysaccharide (LPS) using two approaches.

***In vivo*:** Mice were injected intra-peritoneally with 500 µl LPS (200µg/ml) (E.coli Serotype 0111:B4, Sigma)/ PBS using a 0.5 cc syringe 29 gauge needle (Braun) or 500 µl PBS. Blood was collected from the retro-orbital (RO) plexus using a non-heparinised capillary tube (2x75mm, Superior) under diethyl-ether anaesthesia at the peak of TNFα production (ie. 90 mins post administration).

Ex vivo: Animals were bled via the RO plexus (200µl), and the heparinised (Pharmacare Limited) whole blood split into 2 parts. Each part was mixed and incubated with an equal volume of either PBS/heparin (4U/ml) or PBS/LPS (50ng)/heparin (4U/ml) for 4 hours at 37°C. Serum and supernatant TNFα concentrations were measured by a TNFα-specific sandwich ELISA.

2.1.3 Tail digestion

5 mm tail sections were taken under sterile conditions and digested o/n at 56°C in 1.5 ml eppedorf tubes containing 750 µl lysis buffer [50mM Tris-HCl [pH8], 100mM EDTA, 100mM NaCl, 1% SDS, 0.5mg/ml Proteinase K (20mg/ml)].

2.1.4 DNA extraction from mouse tails

Protein was precipitated from lysates by adding 250µl of a saturated NaCl (6M) solution. This was mixed briefly in an eppendorf shaker and centrifuged in a microfuge at 14000 rpm for 5 mins. 750µl of supernatant was transferred to a new eppendorf containing 300µl chloroform, mixed and centrifuged at 14000 rpm for 30 secs. The upper phase was taken and DNA precipitated by adding 0.6 Vol. cold isopropanol (-20°C). This was centrifuged at 14000 rpm for 5 mins, and the pellet washed with 0.5ml 70% ethanol by vortexing and subsequent centrifugation (5 mins, 14000 rpm). Pellets were dried in a 37°C incubator and dissolved in 0.5ml ddH_2O at 37°C. DNA solutions were stored at -20°C until further use.

2.1.5 PCR reactions

The PCR reactions were carried out in thin walled 0.2ml 8-strip PCR tubes in a PTC 200 Peltier Thermocycler (MJ Research, Massachusetts, USA).

Table 2:Standard PCR Reaction Mix (x1):

DNA sample	2µl
10x Taq Buffer	5µl
DNTP (2.5mM, Promega)	4µl
Primer 1 (6.25µM)	2µl
Primer 2 (6.25µM)	2µl
Taq (5U/µl)	0.05µl
ddH_2O	34.95µl

Primers for use in PCR reactions were synthesised at the Department of Biochemistry, University of Cape Town. 5µl loading buffer (0.25% bromophenol blue, 0.25% xylene cyanol, 50% glucose) was added to 25µl of the amplified products. These were separated by electrophoresis on 1.6% agarose gel (Whitehead Scientific D1 LE) in TBE buffer (44.5mM Tris, 44.5mM boric acid, 1mM EDTA), buffer containing 0.4ml ethidium bromide/100ml (10mg/ml). Bands were visualised using the Gel Doc system (Biorad) and Multianalyst software (Microsoft).

PCR to genotype LBP-/- mice:

Primers:

P1: 5 AgA ggC Atg gTg gCC AgA 3

P2: 5 CCC ACT CCT ggg CTT TgT 3

N1: 5 CTg AAT gAA CTg Cag gAC gA 3

N2: 5 ATA CTT TCT Cgg Cag Gag CA 3'

P1 + P2 amplify the region flanking the Neo cassette

N1 + N2 amplify a region within the Neo cassette

Thermocycling conditions:

1. 94°C 30
2. 61°C 30
3. 72°C 30 35X

PCR products:

WT band (P1 + P2) = 195 bp

KO band (P1 + P2)= 465 bp

Neo band (N1 + N2) = 172bp

(As we were unable to amplify the larger LBP-/- band, we utilised a Neo PCR in combination with the detection of the LBP WT fragment.)

Table 3: Expected result after LBP/Neo PCR

PCR reaction	LBP +/+	LBP+/-	LBP -/-
LBP WT (195)	+	+	-
Neo (172 bp)	-	-	+

2.1.6 Detection of Cytokine and Chemokines by ELISA

The concentration of the cytokines IL-12, IFNγ and TNFα, and the chemokine MCP-1 were determined using sandwich ELISA (Enzyme Linked Immunosorbent Assay).
96 well microtiter ELISA plates (Maxisorp [NUNC]) were coated with 50µl appropriate coating antibodies (see appendix B), diluted in dilution buffer (0.1% BSA/PBS/.02% sodium azide [Merck]) and incubated at 4°C / o/n. Plates were washed three times with PBS and incubated with 150µl blocking buffer (4% BSA/PBS/0.04% sodium azide) for 2 hrs at 37°C to block residual binding sites on the plastic. Plates were next washed 4x with washing buffer (0.05% Tween20 [Sigma], PBS, 0.01% sodium azide) and incubated with 60µl of samples diluted 3-fold in dilution buffer and 60µl appropriate cytokine standards included in 12 three-fold dilutions. This step was incubated o/n at 4°C, plates washed as before and incubated with 100µl of a capture antibody (see appendix) for 2 hrs at 37°C. After washing, either 100µl streptavidin-alkaline phosphatase (1/1000) (for biotinylated secondary antibodies) or an alkaline-phosphatase conjugated antibody was added for 1 hr at 37°C. Plates were developed by incubating with 100µl p-nitrophenylphosphate (Boehringer Mannheim,1 mg/ml in Diethanolamine buffer, see Appendix) and read at 405/492 nm in a microtiter spectrophotometer (Organon, Technika). To stop reactions 50µl 1M NaOH was added.

2.2 Preparation of Infective *Mycobacterium tuberculosis*

2.2.1 Cultivation

Mycobacterium tuberculosis H37Rv was obtained from Prof. G Kaplan, Rockefeller University NY. A sample was removed from a Lowenstein-Jensen slant using a sterile plastic disposable inoculating loop, and deposited into a 50ml sterile screw-capped tissue culture flask (Greiner labortechnik) containing 10 ml of Middlebrook 7H9 Broth [Difco]/ 10% OADC enrichment medium (State Vaccine Institute, Cape Town). Culture flasks were incubated at 37°C in a CO_2 incubator and shaked daily to gently agitate the broth. Incubation proceeded for 1-2 weeks until the culture was very turbid (CFU density of 5x 10^7 to 5x10^8/ ml) and in the mid-late log growth phase.
20 ml from this culture was carefully transferred into a 250 ml sterile screw-capped culture flask (Greiner labortechnik) containing 90 ml Middlebrook 7H9 Broth [Difco]/ 10% OADC

enrichment medium. These culture flasks were further incubated for 1-2 weeks at 37°C in a CO_2 incubator and shaked daily until a similar turbidity was attained.
Aliquots of these mid-late log phase cultures were aseptically prepared by pipetting 1 ml per vial into sterile 2 ml serum vials (Greiner). These aliquots were place into a storage box within a —70°C freezer until further use.

2.2.2 Inoculum Determination- Colony Forming Unit (CFU)

The concentration of bacilli was determined by making 10-fold serial dilutions in 0.9% NaCl/ 0.04% Tween 80, and plating out dilutions of 10^{-2} to 10^{-7} on Middlebrook 7H10 Agar (1.9% 7H10 Agar [Difco], 0.5% glycerol, 10% OADC [oleic acid, dextrose) on 2 compartment plates (90mm Plates, Sterilin). These were incubated at 37°C for 15-18 days and colonies counted using an inverted microscope (Wild M8 Heerbrugg).

2.3 Aerosol Infection of Mice

2.3.1 Preparation of Inoculum for Aerosol Infection

An established procedure was followed when preparing the inoculum (Robert and Orme, 1999). An aliquot of *M.tb* was thawed at room temperature, centrifuged at 4000rpm for 5 mins, and resuspended in a total volume of 6ml 0.9% Saline. The inoculum was sonicated on level 1-2 (4x 5 secs. on/off cycles) to disrupt clumping. To obtain the desired rate of infection, the inoculum was prepared 5 $\log_{10}$ CFU higher than one required delivered into the lungs of the animals (the aerosol machine is programmed to deliver into the lungs approximately 5 $\log_{10}$ CFU lower than the inoculum nebulised) ie. to obtain 100 CFU/lungs, the mycobacterial suspension was prepared at 2.0x 10^6 CFUs/ml in a total volume of 6ml sterile 0.9% saline ($1.0x10^7$ CFU/5ml nebulised) To confirm the inoculum, 10-fold serial dilutions from 10^{-1} to 10^{-7} were prepared and plated on Middlebrook 7H10 agar.

2.3.2 Aerosol Procedure

The aerosol exposure chamber (Middlebrook) was sterilised prior to use with a 3% virkon solution followed by 70% ethanol. The metal basket support/baffle plate and stainless steel mesh exposure basket was placed into the chamber drum. The divisions within the drum were labelled appropriately with the mouse strain, and the mice transferred from their cages into the basket (sexes separated). The basket lid was secured and the perspex chamber lid sealed by firmly snapping the latches. After sealing the chamber, the glass Nebuliser-Venturi was mounted to the compressed air and main air flow fittings, which was secured by 3 clamps. A safety mask was placed over the face for the rest of the procedure. Carefully, the screw cap on the nebuliser was removed and 5ml of the inoculum added into the bottom of the venturi using a 5ml syringe fitted with an 18-gauge needle. After screwing the lid closed, the instrument was switched on including the UV lamp and computer.
The program to be entered for aerosolising mice was as follows:

(i) Preheating time 15 minutes
(ii) Nebulising time 40 minutes
(iii) Cloud decay 40 minutes
(iv) Decontamination 15 minutes

The preheating time is to enable the incinerator to achieve its core temperature of 790°C in order to decontaminate the exhaust air. During the nebulisation cycle the compressed air is activated and passes through the venturi of the nebuliser to create droplet nuclei containing bacilli. These droplet-nuclei are carried into the chamber containing the animals. The third cycle is cloud decay in which the aerosol chamber is purged with fresh air and the bacterial mist dissipated. During the final cycle the UV lamps are switched on to decontaminate the top surfaces of the basket. Once the instrument had initiated the Preheat cycle , the Main Air Flowmeter should indicate 60 cubic feet/hour (CFH), and adjusted with the control valve if necessary.
When the nebulising cycle starts, the Compressed Air Flowmeter should be at 10 CFH, and adjusted if required. The room containing the chamber was then vacated until the process ended (110 minutes), and the door appropriately marked to prevent intrusion. After completion of the cycle, the instrument was switched off, the lid opened, and the mice returned to their cages. All the contaminated components were wrapped up, sterilised by autoclaving, scrubbed clean and then autoclaved once more.

2.3.3 Determination of Initial Pulmonary Infection (Day 1)

To determine uptake of mycobacteria into the lungs of the mice, 5 animals were sacrificed by cervical dislocation one day after aerogenic challenge. Entire lungs were removed and immediately placed into sterile tubes containing 1ml of 0.9% NaCl/0.04% Tween80 solution. After all necropsies were completed, individual lungs were transferred into sterile 10ml perspex mortar and homogenised with a pestle secured in a drill (Black and Decker KD574CRE, 680W). Lung homogenates were plated in duplicate volumes of 100ul and 200ul on Middlebrook 7H10 agar in duplicate, incubated at 37°C for 15-18 days, and CFUs enumerated.

2.4 Phenotypic Analysis

2.4.1 Mortality Studies

To assess the susceptibility of mice, groups of 5-10 sex-matched mice between the age of 8-12 weeks were challenged aerogenically with *M.tb* H37Rv. Mice were sacrificed as in 2.3.3 to determine the initial pulmonary infection. Animals were monitored regularly and weighed on a weekly basis to assess the progression of the disease. Animals succumbing to infection were discarded and the time post-infection recorded.

2.4.2 CFU determination in organs

To determine the growth of the mycobacteria in the animals, groups of 3-4 mice from each group were sacrificed at various time points. Livers, spleens and lungs were removed and immediately placed into sterile tubes containing 4ml of 0.9% NaCl/ 0.04% Tween80 solution. After all necropsies were completed, individual organs were transferred into sterile 10 ml perspex mortar and homogenised with a pestle secured in a drill (Black and Decker KD574CRE, 680W). 100ul of organ homogenates were plated in duplicate on Middlebrook 7H10 agar, incubated at 37°C for 15-18 days, and CFUs enumerated

2.4.3 Histology of Paraffin Wax Embedded Tissue

A section of the liver, spleen and lung was removed from each mouse sacrificed, and placed immediately in a solution of 4% buffered Formaldehyde (Merck). These sections were left in solution for 2 days to ensure killing of bacilli. Sections were then processed o/n, embedded in paraffin wax, and cut to 2µm with a microtome .

2.4.3.1 Haematoxylin and Eosin staining (HE)

Tissue sections were dewaxed o/n by incubating at 56°C in an oven. The next day, tissue sections were rehydrated by passing them sequentially through: 2x xylol, 2x 100% ethanol, 2x 96% ethanol, 2x 70% ethanol, and ddH_2O. Slides were placed in a haematoxylin solution for 8 minutes and then washed in ddH_2O for 1-2 minutes. The excess staining was removed by immersion in 1% acid alcohol for 10 seconds, and the blue colour retrieved by leaving the slides in ddH_2O for 30 minutes. The slides were next placed in 1% eosin for 2 minutes, washed in ddH_2O, and dehydrated by passing through 2x 10% ethanol, 2x 96% ethanol and 2x 100% ethanol. The sections were finally immersed in xylol, mounted with Canada Balsam, and covered with a coverslip.

Materials

Mayer s Haematoxylin

1g haematoxylin

50g ammonium (or potassium alum)

0.2g sodium iodate

1g citric acid

1l ddH_2O

Acid alcohol

1% HCl in 70%ethanol

2.4.3.2 Ziehl-Neelsen Staining (ZN)

Tissue sections were dewaxed o/n by incubating at 56°C in an oven. The next day, passing them sequentially through 2x xylol, 2x 100% ethanol, 2x 96% ethanol, 2x 70% ethanol, and ddH2O rehydrated sections. Slides were placed on a staining rack and flooded with 6% carbol

fuschin, flamed until steaming and then left for 5 minutes. The flaming-cooling step was repeated as before, and followed by a washing step in ddH_2O. Sections were rinsed in 1% acid alcohol until excess colour removed, washed in ddH_2O, and immersed in 25% H_2SO_4 for 20 minutes. Slides were washed in running ddH_2O for 10 minutes to remove acid and counterstaining was performed in Loeffler s methylene blue for 30 seconds. Sections were washed a final time, dehydrated through to xylol and mounted in Depex mounting medium (Merck).

Materials

Carbol Fuschin Solution

A 6% stock solution of carbol fuschin is prepared in 100% alcohol. For use in staining, 10 ml stock carbol fuschin is added to 90 ml phenol and filtered.

Loeffler s Methylene Blue

A stock solution is prepared by dissolving 0.8% methylene blue in 100% alcohol. For use in staining, 30 ml stock solution and 1 ml 1% potassium hydroxide (in ddH_2O) were added to 99 ml ddH_2O. The solution was filtered before use.

2.4.3.3 Antigen retrieval and Immunohistochemistry (IHC)

To expose the epitopes masked by the paraffin wax, a retrieval method was utilised. Slides were incubated o/n at 56°C to melt the wax and the following day rehydrated by passing through 2x 100% ethanol, 1x 96% ethanol, 2x 70% ethanol and ddH_2O. To demask the epitopes, sections were microwaved in citrate buffer on medium setting for 2x 5 min., and then left in the buffer to cool to room temperature for 20 min. Sections were next fixed in acetone for 10 min., followed by 15 min. air-drying. Endogenous peroxidase activity was blocked by incubating in 1% H_2O_2/ methanol for 30 mins, followed by a wash with 1x PBS. To block endogenous biotin, sections were incubated in 0.1% avidin for 30 min., avidin shaken off, and then incubated in 0.01% biotin for 20 min. Blocking was performed for 30 min. in 1.5% serum/ PBS, serum shaken off and sections incubated o/n at 4°C with 50µl of the primary antibody at a previously determined concentration. The following day, sections were washed with 1x PBS and incubated with the appropriate secondary antibody for 30 mins. ABC vector kit was added to the sections for 30 min., followed by a washing, and then a 10 min. incubation with the DAB substrate (1ml buffer to 1 drop chromagen) (Dako).

Sections were washed in running ddH_2O, incubated in 1% $CuSO_4$ for 2 min. and then washed again for 2 min. in running ddH_2O. Sections were counterstained in Mayer s haematoxylin for 4 min. and washed in running H_2O. Sections were dehydrated by passing through 2x 70% ethanol, 1x 96% ethanol, 2x 100% ethanol, 2x xylene. Finally, sections were mounted in Entellen and covered with a coverslip.

Materials
Entellan (Merck)

Citrate buffer pH 6:
Solution A- 1.05g citric acid in 50ml ddH_2O (0.01M)
Solution B- 2.94g sodium citrate in 100ml ddH_2O (0.1M)
Working solution — 9ml A + 41ml B in 500ml ddH_2O

2.4.4 Bronchoalveolar Lavage (BAL)

2.4.4.1 Quantification of cytokine/chemokine levels in BAL fluid

Mice were administered a lethal dose of anaesthetic intra-peritoneally (50mg/ml Ketamine hydrochloride/ 2% Rompun). The mouse to be lavaged was then pinned to the dissecting board, and its trachea exposed in a sterile manner by making a small incision in its neck. The skin, fatty tissue and salivary gland was carefully cut away, trying to avoid severing the surrounding blood vessels. The membrane surrounding the trachea was removed and to support it, a 21-gauge needle inserted from the underside. The dissecting board was elevated to ensure flow of lavage fluid into the lungs. A 22 gauge cannula (Introcan 0.9x 25mm, Braun) was inserted into the trachea, and when firmly in place, the needle removed from the cannula. A 1ml syringe was attached to the end of the cannula, and the lungs lavaged twice with 350µl of ice cold PBS solution (5 aspirations). The lavage fluid recovered was placed in an eppendorf tube and stored on ice. The lungs were lavaged a further 3 times with 900µl PBS (5 aspirations), and the fluid recovered placed in 14ml conical tubes (Sterilin). The lavage fluid in the eppendorfs was centrifuged at 2000 rpm for 5 mins, and 100µl aliquots of the supernatant prepared. These aliquots were stored at —70°C until further use. For the detection of cytokines/ chemokines, appropriate aliquots were thawed and used in sandwich ELISAs as described above in *2.1.6.*

2.4.4.2 Differential count of cells in BAL fluid

The conical tubes containing the remaining BAL fluid was centrifuged at 2000 rpm for 5 mins, the cell pellet obtained, pooled with the eppendorf pellet, and resuspended in a total volume of 1ml. Viable cell numbers were counted with trypan blue (1:1), (0.4%, Sigma), diluted to 2-3x 10^5 cells/ml, and duplicate 50µl volumes placed in 8 well teflon coated microscope slides (6mm, Highveld Biological). The slides were left at room temperature to air-dry, stained with the RapiDiff kit (Clinical Sciences Diagnostics) by immersing the slides briefly in RapiDiff fixative, Rapidiff solution 1 (Eosin in Phosphate Buffer), RapiDiff Solution 2 and a final rinse with ddH_2O. Differentials were assessed after placing a coverslip over the slide. Cell percentages were determined by counting 100 cells/well, (n=4 mice per group). The cell free supernatant was frozen for cytokine or chemokine ELISA determinations.

2.4.5 Quantification of Cytokine/ Chemokines in lung homogenates

Mice were sacrificed, entire lungs removed, and an equal lung mass placed in 1ml of ice cold PBS solution. The contents were transferred into sterile 10 ml perspex mortars (kept on ice) and homogenised with a pestle (4x 10 second cycles) using the Black and Decker Drill on high (setting of six). Homogenates were centrifuged at 14000 rpm, supernatants aliquotted in 100µl volumes, and stored at —70°C until further use. Prior to use in ELISA, aliquots were thawed, centrifuged at 14000 rpm, and the supernatants used for cytokine/ chemokine quantification.

3. Results

3.1 The Role of TLR4 in the Host Immune Response to a *M.tuberculosis* Infection

3.1.1 Phenotyping the TLR4 mutant C3H/HeJ

The TLR4 mutant was phenotyped by its hyporesponsiveness to *LPS in vivo* and *ex vivo*.

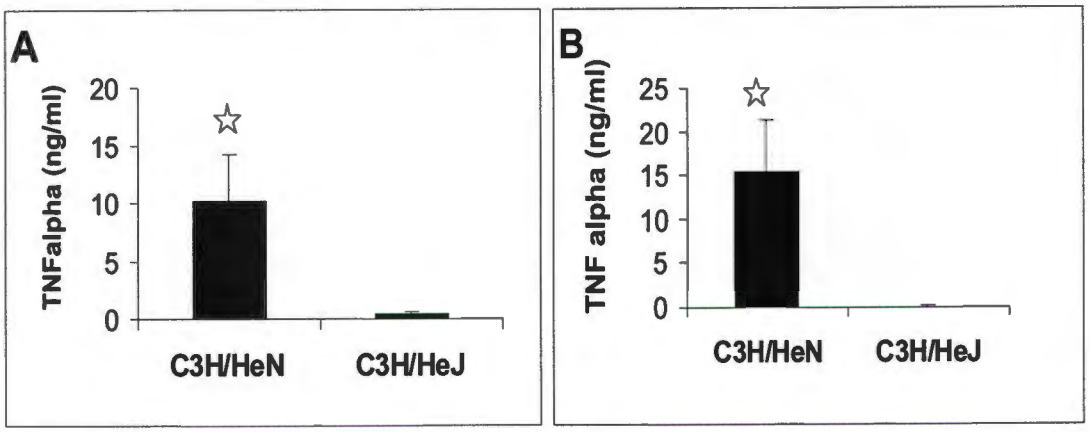

Fig. 3.1:Measurement of TNFα production in response to LPS (n=4 mice/ group)
A: (*in vivo*): TNFα measured 90 min. following administration of 100μg LPS i.p
B: (*ex vivo*): TNFα measured in supernatant of whole blood cells stimulated with 50ng LPS (4 hrs, 37°C)
(☆ P < 0.05). (PBS administered as a negative control resulted in no detectable levels of TNFα (data not shown)).

The C3H/HeN mice, which have the wild-type allele of the TLR4 gene, display the classical *in vivo* symptoms of endotoxic shock in response to LPS (ie. weight loss, ruffled coat, diarrhoea, immobility and mortality). The substantial production of TNFα in response to LPS was observed in the C3H/HeN mice, but not in the C3H/HeJ mice (*in vivo* Fig. 3.1A). The C3H/HeN-derived whole blood (WB) cells are acutely sensitive to LPS and release an ample amount of TNFα in response (*ex vivo* Fig. 3.1B). The C3H/HeJ mice, which have a mutant allele of the TLR4 gene are protected from the endotoxic shock and do not manifest any of the symptoms that afflict the C3H/HeN mice. Surprisingly, the C3H/HeJ mice do produce TNFα in response to LPS, but at a level much lower than the C3H/HeN mice (Fig. 3.1A)
This apparent responsiveness by the C3H/HeJ mice to LPS is probably due to trace amount of contaminants in the LPS/ PBS solution (personal communication with C.Galanos).
This hyporesponsiveness to LPS is confirmed *ex vivo* by the diminished production of TNFα by C3H/HeJ-derived whole blood cells (Fig.3.1B). These results confirm the phenotype of the C3H/HeJ mice.

3.1.2 Mortality of the Tlr4 mutant C3H/HeJ

To assess the susceptibility of the TLR4 mutants to an *M.tb* infection, 5 female C3H/HeN and C3H/HeJ mice (8-12 weeks old) were challenged aerogenically. The mice were monitored regularly, weighed weekly and mortality was recorded.

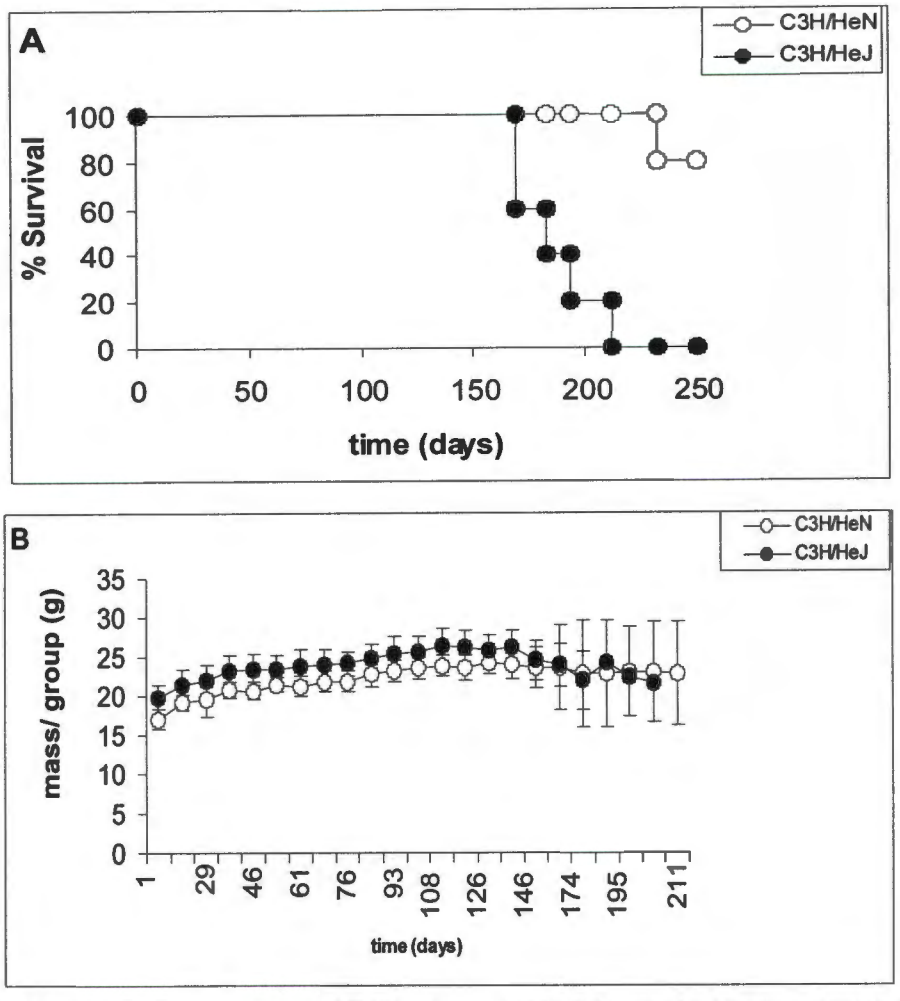

Fig. 3.2: (A) Mortality study of C3H/HeN mice vs. C3H/HeJ mice infected aerogenically with *M.tb* H37Rv (dosage at day1 = 50-100 CFU/lung, n=5 mice/ group). (B) Mean weight of C3H/HeN vs. C3H/HeJ mice during the infection (n=5 mice/ group).

Only one of the C3H/HeN mice succumbed to the infection up to the time observed, whereas the C3H/HeJ mice slowly deteriorated and all eventually died between 5 and 7 months (Fig. 3.2A). The mean weight of the C3H/HeJ mice, which was slightly greater than the C3H/HeN mice initially, decline from day 146 (Fig. 3.2B), concomitant with these mice succumbing to *M.tb* infection.

3.1.3 CFU study of Tlr4 mutant C3H/HeJ

To investigate the progression of the disease with respect to the mycobacterial load, livers, spleens and lungs were removed and CFU assays performed.

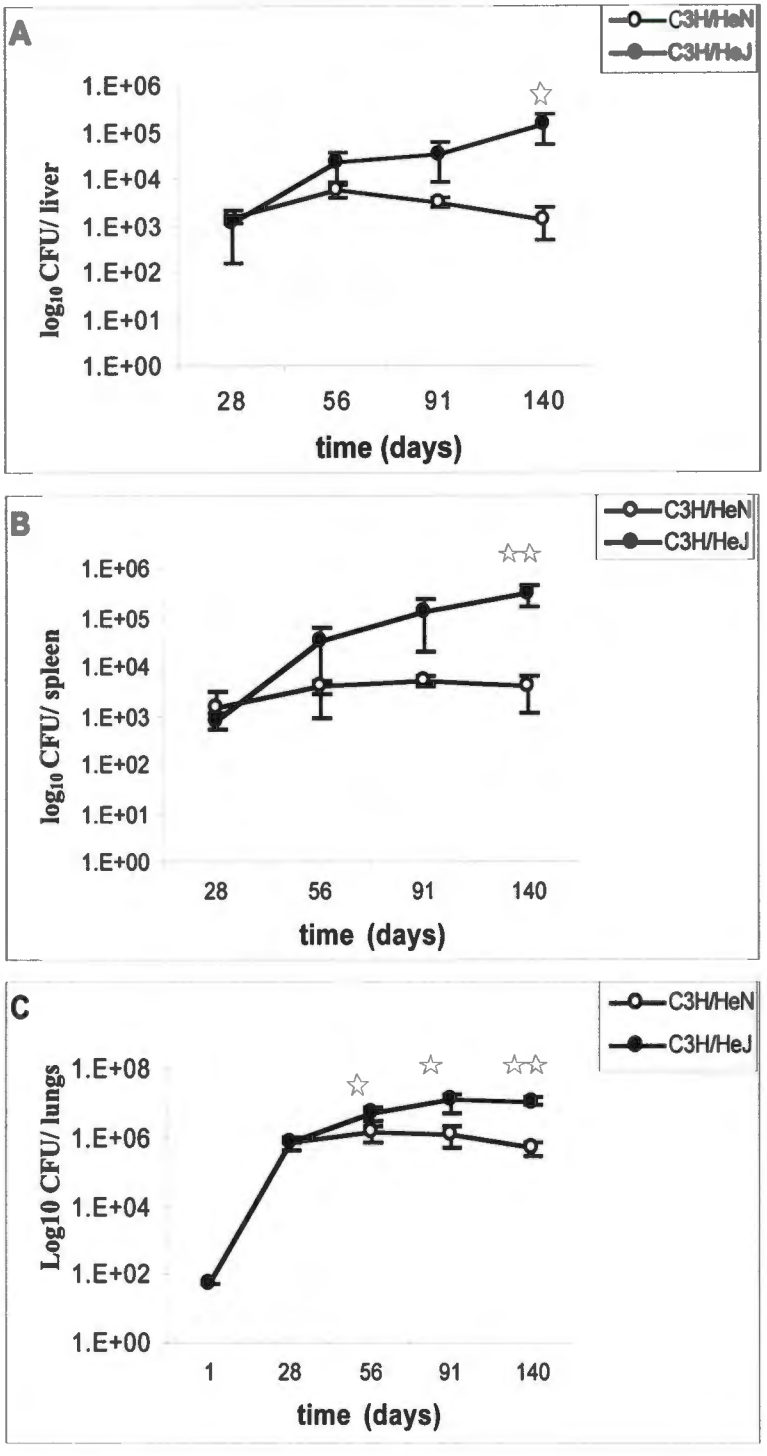

Fig. 3.3: Mycobacterial load assessed in the liver (A), spleen (B) and lungs (C) by CFU assay. Data expressed as the mean number of viable bacteria, and standard deviations indicated with the vertical bars. (n= 3-4 mice/ group, ☆ $p<0.05$, ☆☆ $p<0.01$ using the Student's t-test).

The initial exposure of these mice was determined to be approximately 100 CFU/ lungs at day one. CFU was not detectable in the liver and spleen at day one (data not shown). Fig. 3.3 demonstrates that the C3H/HeN mice were able to control the *M.tb* infection in the liver, spleen and lungs. The number of viable bacilli in the lungs decline gradually two months post-infection, and insignificant growth is noted extra-pulmonarily. In contrast to this, the C3H/HeJ mice appear to be impaired in their ability to control the *M.tb* infection. The pulmonary infection in these two groups diverges after one month, and a significant progression is noted in the lungs of the C3H/HeJ mice (Fig. 3.3C). Dissemination from the lungs occurs at the same rate initially (at 1 month), but the effective control of infection in the lungs, liver and spleen of the C3H/HeN mice is clearly absent in C3H/HeJ mice (Fig. 3.3A, Fig. 3.3B and Fig. 3.3C).

3.1.4 Analysis of organ weights of the C3H/HeN vs. C3H/HeJ mice

During necropsy, the masses of the liver, spleen and lungs were recorded and later expressed as a ratio of the respective mouse body weight (BW). These calculations give an indication of the developing inflammatory response with respect to cellular recruitment within the organs. (The average group mass remained stable for most of the experiment, thus the differences noted between the ratios (organ weight/ body weight expressed as a percentage) can be attributed to inflammatory processes and not necessarily BW loss).

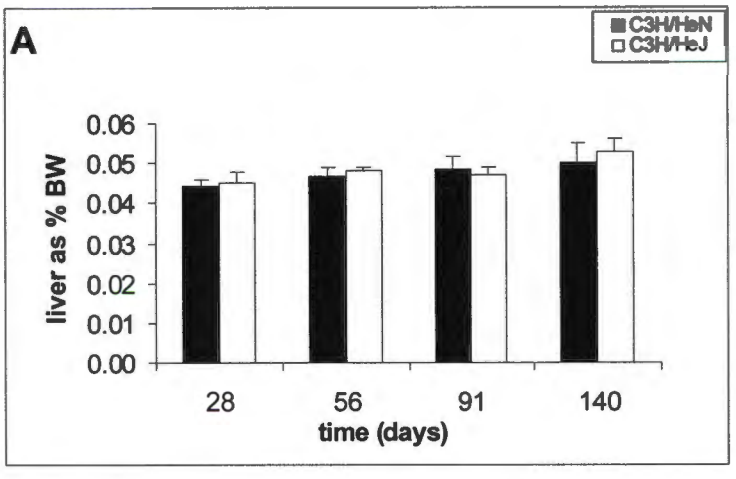

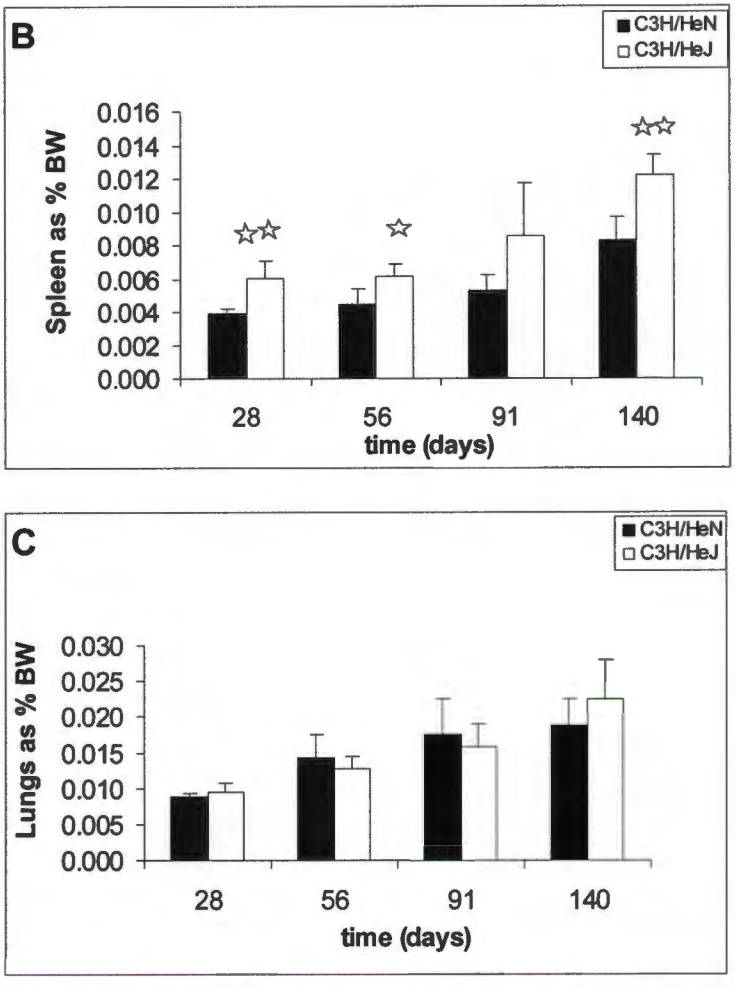

Fig. 3.4: Analysis of organ weights: body weight (BW) ratio in the C3H/HeN vs. C3H/HeJ mice
(A) liver expressed as a ratio of body mass, (B) spleen expressed as a ratio of body mass, (C) lungs expressed as a ratio of body weight (n=4 mice/ group, ☆$p< 0.05$, ☆☆$p<0.01$ using the student's t-test).

There is no significant difference between the ratios of the liver (Fig. 3.4A) and the lungs (Fig. 3.4C), but the spleen of the C3H/HeJ mice are significantly more inflamed than those of the C3H/HeN mice (Fig. 3.4B)

3.1.5 Histological analysis of C3H HeN and C3H HeJ mice infected with M.tuberculosis

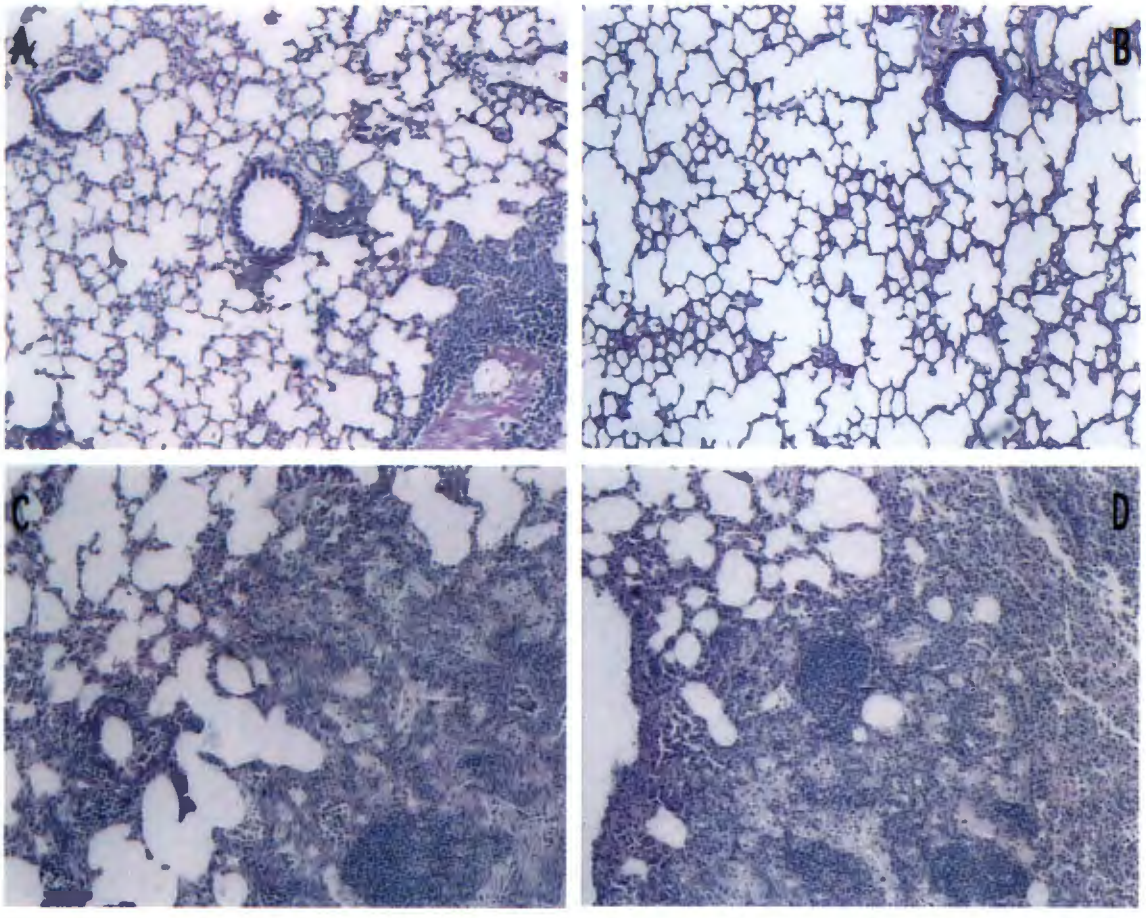

Fig 3.5: Microscopic alterations in lungs of C3H/HeN (left panels) and C3H/HeJ mice (right panels) 28 days (A, B) and 140 days (C, D) post aerosol *M.tb* infection using HE stain (histology performed on 2 sections per mouse, 3-4 mice per group)

The Haematoxylin and Eosin (HE) stain revealed that there was comparable inflammation at 28 days post-infection in the lungs of the C3H/HeN mice (Fig. 3.5A) and the C3H/HeJ mice (Fig. 3.5B), but a more prominent neutrophil presence in the C3H/HeJ lungs. At 140 days post-infection, more congestion was noted in the lungs of the C3H/HeJ mice (Fig. 3.5C) resulting in less airspace than the C3H/HeN lungs (Fig. 3.5D). The level of granulomata were comparable in the lungs of the two groups, but an increased lung parenchymal infiltration by neutrophils was observed in the C3H/HeJ mice upon examination of histological sections (data not shown).

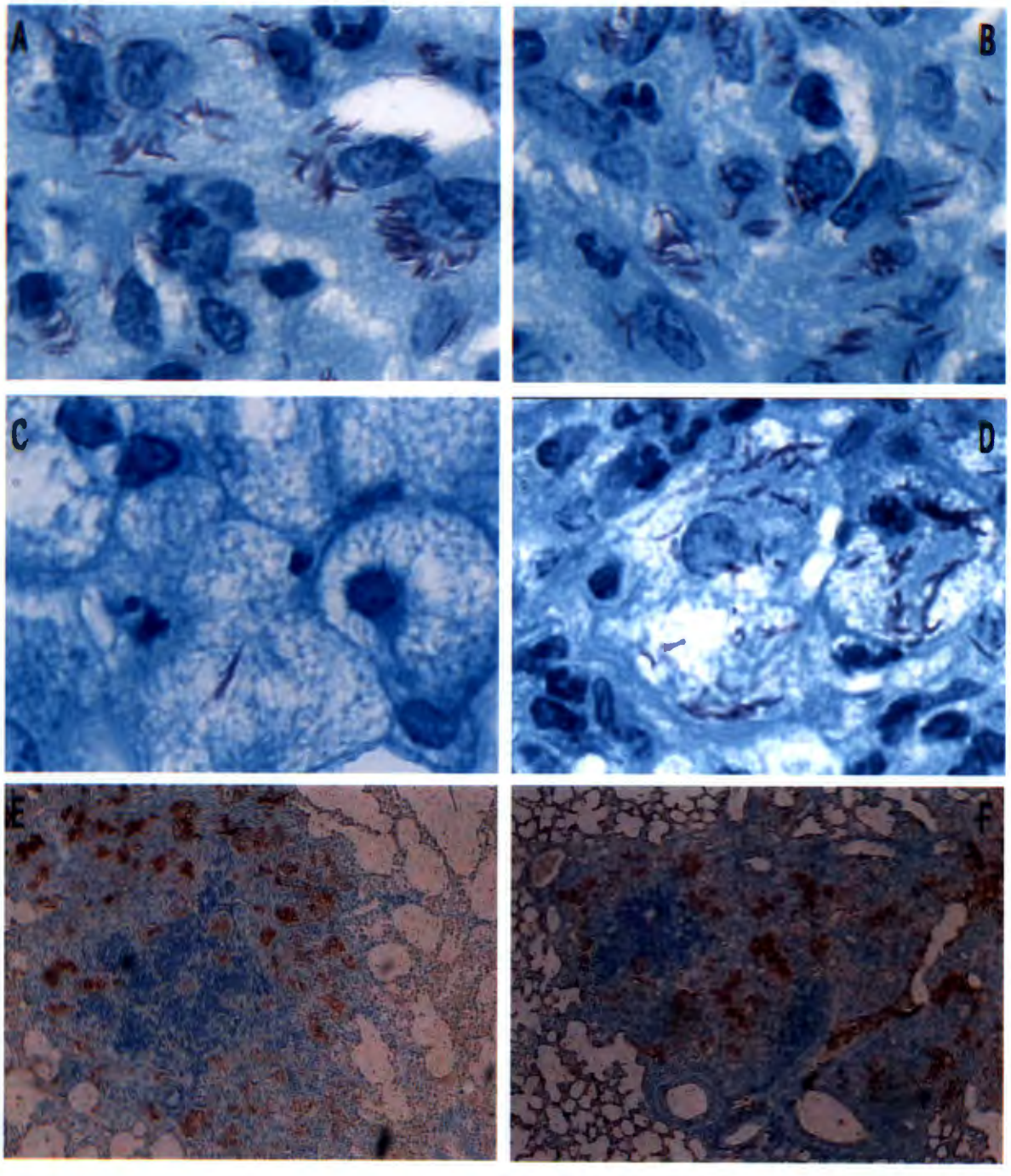

Fig. 3.6: ZN stain for acid-fast bacilli (A-D) and iNOS2 (E,F) in lungs of C3H/HeN (left panels) and C3H/HeJ mice (right panels) 28 days (A,B), 140 days (C,D) and 56 days (E,F) post aerosol *M.tb* infection (histology performed on 2 sections per mouse, 3-4 mice per group)

The ZN stain revealed that at 28 days post-infection, the level of acid-fast bacilli (AFBs) was similar in the two groups of mice (Fig. 3.6A and Fig. 3.6B). However, at 140 days, while AFBs were easily noticed in primarily foamy macrophages of the C3H/HeJ lungs (Fig. 3.6D), they were virtually undetectable in the C3H/HeN lungs (Fig. 3.6C). The iNOS2 stain revealed

that at 2 months post-infection, there was no difference in the expression of iNOS2 between the two groups.

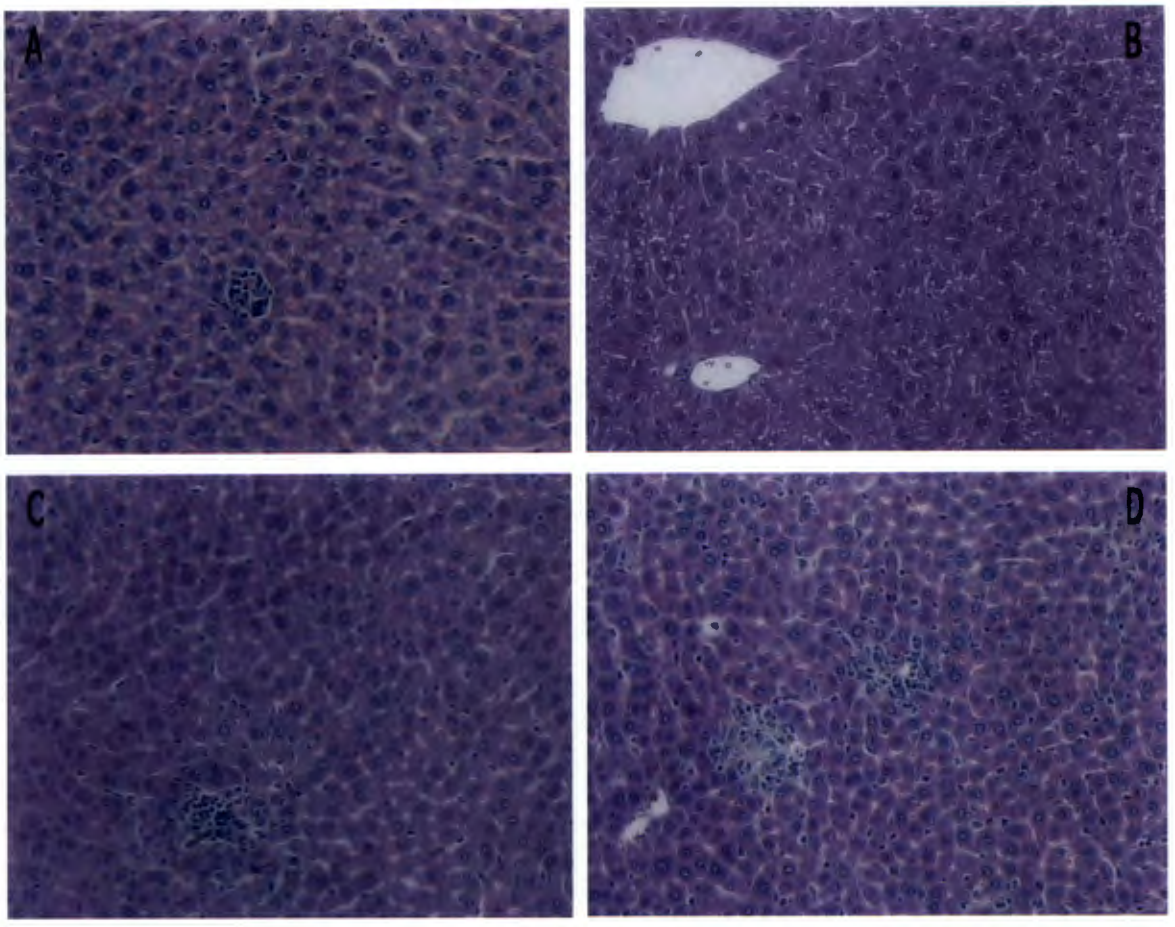

Fig. 3.7: Microscopic alterations in livers of C3H/HeN (left panels) and C3H/HeJ (right panels) mice 28 days (A,B) and 140 days (C,D) post aerosol *M.tb* infection by HE stain (histology performed on 2 sections per mouse, 3-4 mice per group).

The HE stain in the liver revealed that at 28 days post-infection there were few diffuse granulomatous structures in the livers of the C3H/HeN mice (Fig. 3.7A) and C3H/HeJ mice (Fig. 3.7B). At 140 days post-infection, there were more prominent hepatic granulomata in the C3H/HeJ mice (Fig. 3.7D) than in the C3H/HeN mice (Fig. 3.7C) (about five-fold more granulomata in the C3H/HeJ livers, data not shown).

3.1.6 Analysis of BAL cells from C3H/HeN and C3H/HeJ mice

Bronchoalveolar lavage (BAL) was performed on C3H/HeN and C3H/HeJ mice 4 weeks after aerogenic challenge with *M.tb,* BAL cells retrieved from the lavages were stained with a RapiDiff kit and counted to determine the type of cells recruited into the alveolar spaces. Naïve mice were analysed to determine the baseline levels (data not shown).

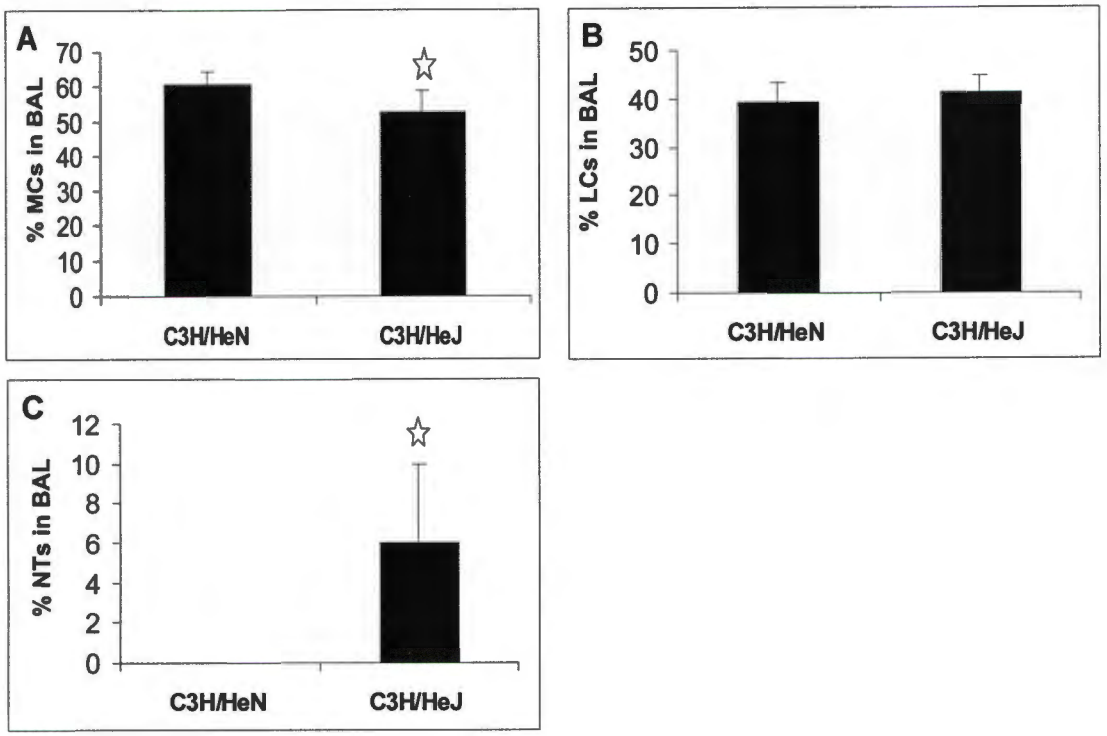

Fig.3.8: Differential counts of BAL cells from C3H/HeN and C3H/HeJ mice 4 weeks into a pulmonary *M.tb* infection. (A) % macrophages in the BAL, (B) % Lymphocytes in the BAL and (C) % neutrophils in the BAL) (n=4 mice/ group☆ p< 0.05 by student's t-test). MCs = macrophages, LCs = lymphocytes, NTs = neutrophils.

The aerogenic *M.tb* infection of these mice was determined to be 300 to 350 CFU per lungs at day 1. The C3H/HeN mice had a significantly larger proportion of macrophages than the C3H/HeJ mice did 4 weeks post-infection (Fig. 3.8A), but the lymphocyte population appeared to be comparable (Fig 3.8B). Interestingly, there was a significant population of neutrophils recruited into the alveoli of the C3H/HeJ mice at this time point, which did not occur in the C3H/HeN lungs (Fig. 3.8C). This data concurs with the histological finding of increased lung parenchymal infiltration by neutrophils in the C3H/HeJ mice (data not shown).

3.1.7 Analysis of cytokine/ chemokine production in BAL fluid of C3H/HeN vs. C3H/HeJ mice

Bronchoalveolar lavage (BAL) was performed on C3H/HeN and C3H/HeJ mice 4 weeks after aerogenic challenge with *M.tb.* BAL fluid was analysed by ELISA to determine the concentration of cytokines and chemokines in the alveolar spaces.

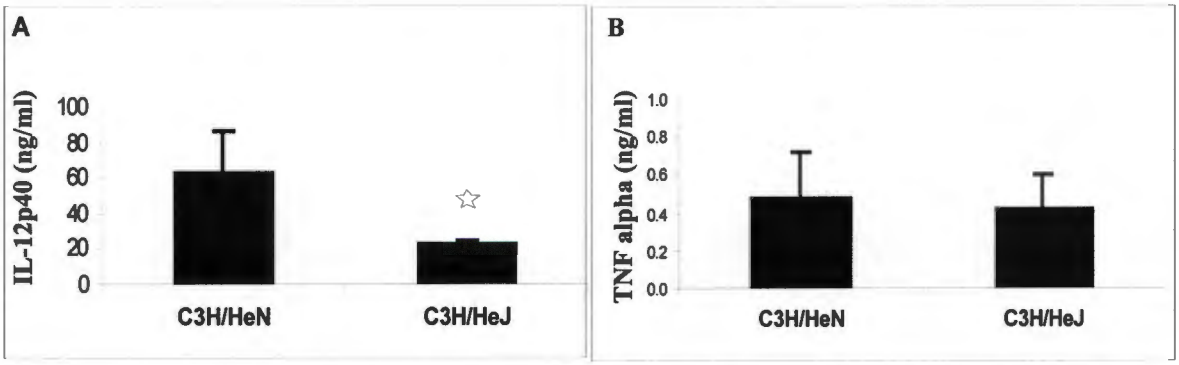

Fig. 3.9: Measurement of cytokine production by ELISA in bronchoalveolar fluid (BAL fluid) at 4 weeks following infection with *M.tb.* (A) IL-12p40 (ng/ml), (B) TNFα (ng/ml). (n=4 mice/ group ☆p <0.05 using student's t-test)

The production of pro-inflammatory IL-12p40 was significantly reduced in the BAL fluid of the C3H/HeJ mice in comparison to the C3H/HeN mice (Fig. 3.9A). The level of TNFα measured in the C3H/HeJ mice was also reduced, but not significantly (Fig. 3.9B). The T lymphocyte and monocyte chemoattractant chemokine, MCP-1, was not detectable in the BAL fluid at this time point (data not shown). IFNγ was also measured in the BAL fluid, and found to be reduced in the C3H/HeJ mice, but not significantly.

3.1.8 Analysis of Cytokine/Chemokine Production in Lung Homogenates of C3H/HeN vs. C3H/HeJ

Lungs derived from C3H/HeN and C3H/HeJ mice 4 weeks post *M.*tb infection were homogenised, centrifuged, and the supernatant analysed for the presence of cytokines/ chemokines. This technique enables the measurement of cytokines/chemokines produced within the entire lung environment, whereas BAL is restricted to measurement within the alveolar spaces.

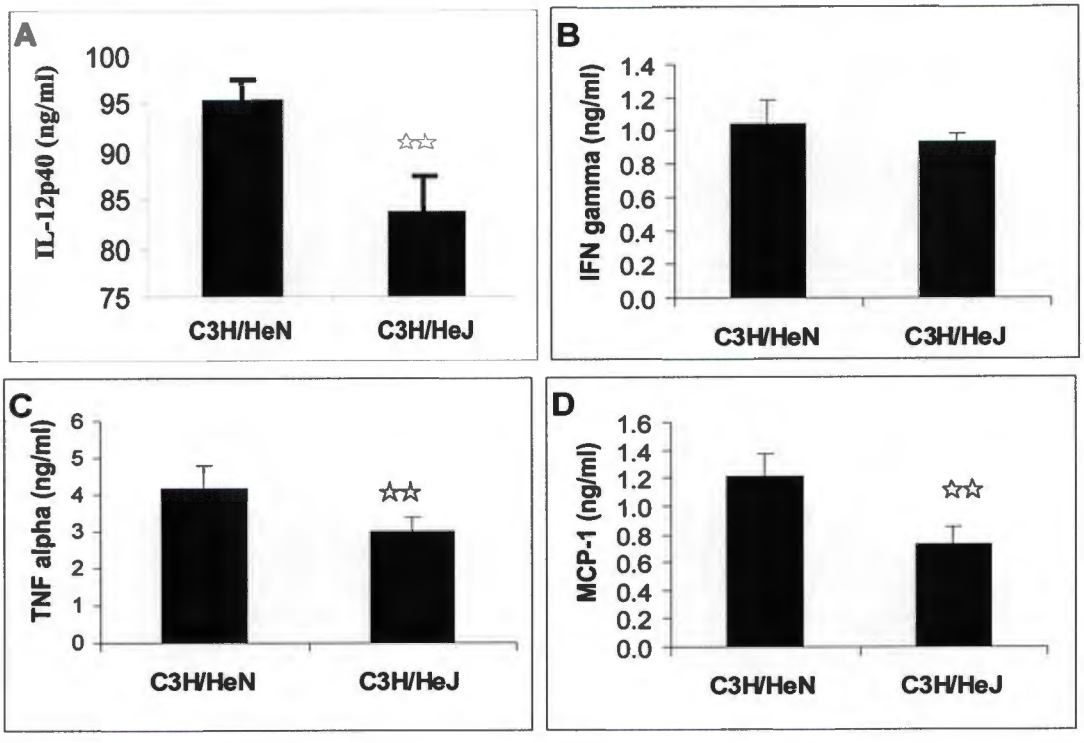

Fig. 3.10: Measurement of cytokines/ chemokines in the lung homogenates 4 weeks post-infection (A) IL-12p40 (ng/ ml), (B) IFNγ (ng/ ml), (C) TNFα (ng/ ml), (D) MCP-1 (ng/ ml) (n=4 mice/ group, ☆ $p<0.05$, ☆☆ $p<0.01$ using student's t-test).

The cytokines IL-12 and TNFα were significantly reduced in the lung homogenates of C3H/HeJ mice when compared to the C3H/HeN mice (Fig. 3.10A and 3.10C).

The level of IFNγ in the C3H/HeJ lung homogenates was lower than in C3H/HeN homogenates, but not significantly (Fig. 3.10B). The monocyte and T lymphocyte chemokine MCP-1 was significantly lower in C3H/HeJ mice than C3H/HeN mice (Fig. 3.10D).

TLR4 appears therefore to play a significant role in the host response to *M.tb* infection. In the absence of TLR4, mice succumb to the infection with a two log higher CFU load in the liver and spleen, and a significantly higher lung load. Reduced resistance appears due to a reduced induction of pro-inflammatory cytokines.

3.2 Preliminary Study: The Role of Lipopolysaccharide Binding Protein (LBP) in *M.tuberculosis* Infection

As the endotoxin response system is composed of primarily CD14, LBP and TLR4, and since we demonstrated the importance of TLR4 in *M.tb* infection, we were interested whether the absence of other components of this system resulted in a similar phenotype. We therefore investigated the role of LBP (CD14-deficient mice were not available for this study).

3.2.1 Genotyping of LBP-/- mice

The LBP genotype was identified by a PCR reaction which detected the presence/absence of the LBP WT allele (Fig. 3.11A) in combination with a Neo PCR (Fig. 3.11B)

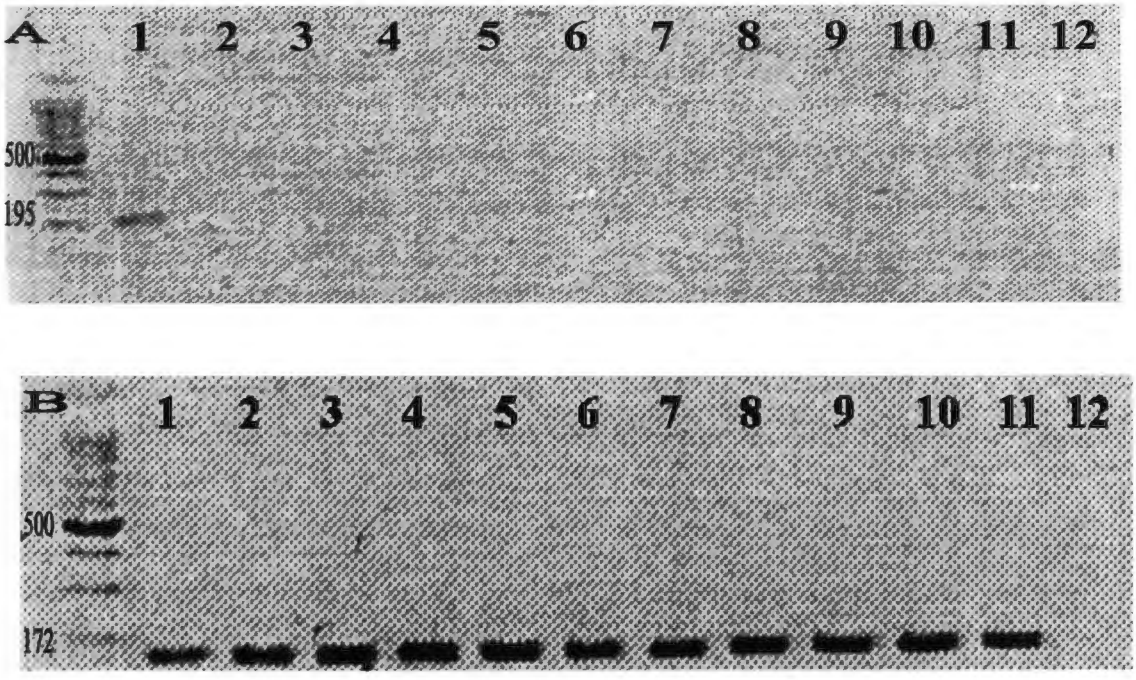

Fig. 3.11: Genotyping of LBP-/- mice.

(A) Amplification of LBP wild-type allele (195 bp)

(B) Amplification of Neo cassette (172 bp)

Lane 1 = +/- mouse , Lanes 2-11 = -/- mice , Lane 12 = negative control

The genetic identity of the LBP mutants was thus confirmed by PCR.

3.2.2 Phenotyping of LBP-/- mice

The LBP mutants were also phenotyped by their hyporesponsiveness to LPS. As with the C3H/HeJ mice, this was done both *in vivo* and *ex vivo*.

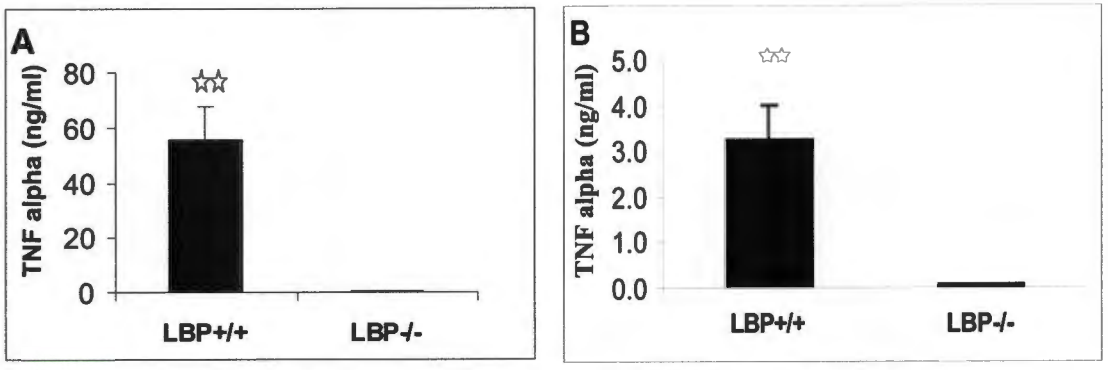

Fig. 3.12:Measurement of TNFα production in response to LPS (n=4 mice/ group)

A: (*in vivo*): TNFα measured 90 min. following 100μg LPS i.p

B: (*ex vivo*): TNFα measured in supernatant of whole blood cells stimulated with 50ng LPS (4 hrs, 37°C) ($p^{☆☆} < 0.01$). (PBS administered as a negative control resulted in no detectable levels of TNFα (data not shown)).

The LBP+/+ mice produced copious amounts of TNFα at 90 minutes in response to LPS challenge i.p (Fig. 3.12A), displayed the symptoms of endotoxic shock, and eventually succumbed. In contrast to this, the LBP-/- mice were protected from shock and produced insignificant TNFα in response to the LPS (Fig. 3.12A). This phenotype was confirmed by the *ex vivo* findings that the LBP-/- mice-derived whole blood cells were insensitive to LPS stimulation, but the LBP+/+ derived cells were LPS responsive (Fig. 3.12B).

3.2.3 Mortality Study of LBP-/- mice

To assess the susceptibility of the LBP-/- mice to an *M.tb* infection, six female LBP+/+ and six LBP-/- mice (8-12 weeks old) were challenged aerogenically. The mice were monitored regularly, weighed weekly, and mortality recorded.

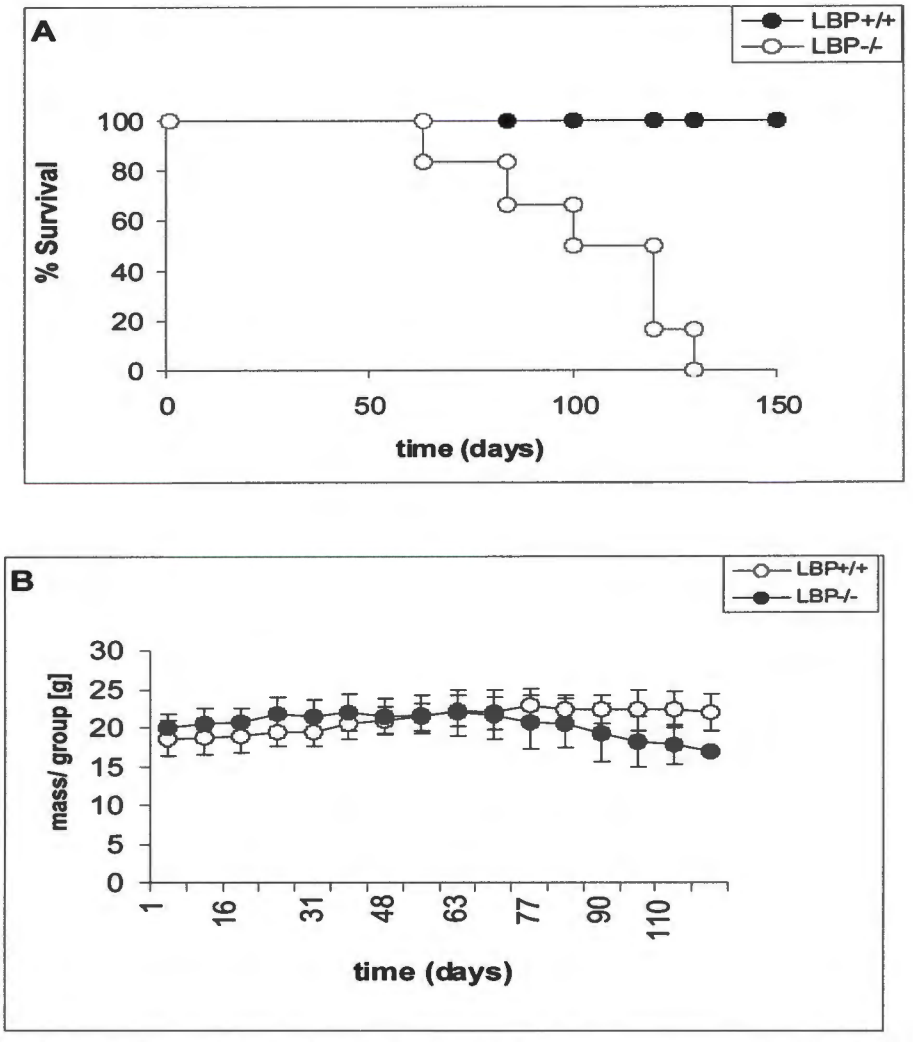

Fig. 3.2: (A) Mortality study of LBP+/+ vs. LBP-/- mice infected aerogenically with *M.tb* H37Rv (dosage at day1 = appro. 100 CFU/lung, n=5 mice/ group). (B) Mean weight analysis of LBP+/+ and LBP-/- mice (n=6 mice/ group).

The LBP+/+ mice survived the duration of the experiment, but the LBP-/- mice succumbed to the *M.tb* infection between 9 and 19 weeks (Fig. 3.11A). The average mass of the LBP+/+ mice remained stable, whereas the mass of the LBP-/- mice declined steadily from 9 weeks onwards (Fig.3.11B).

3.2.4 CFU study of LBP+/+ vs. LBP-/- mice

To investigate the progression of the disease with respect to the mycobacterial load, liver, spleen and lungs were removed and CFU assays performed.

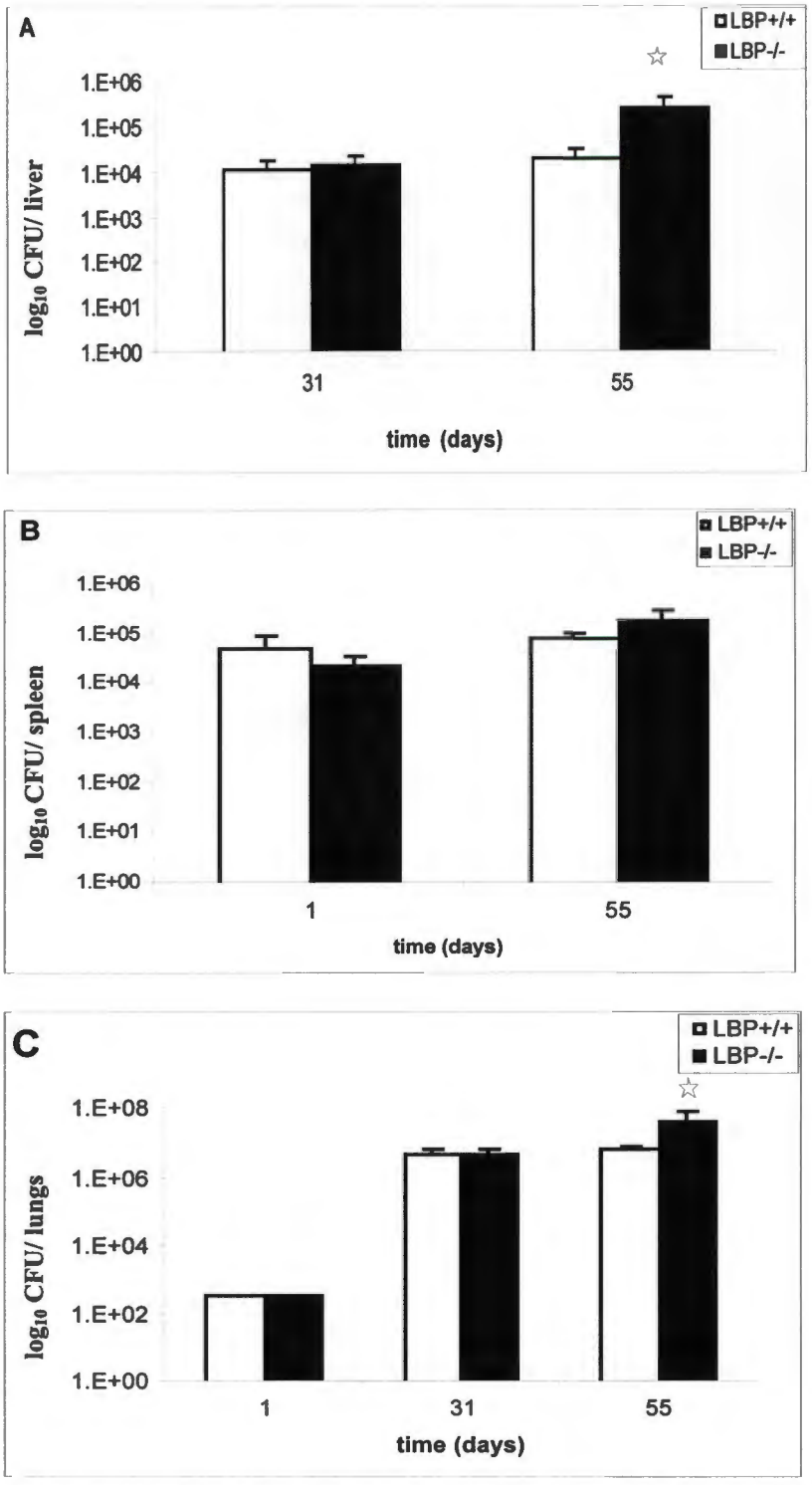

Fig. 3.14: Mycobacterial load assessed in the liver (A), spleen (B) and lungs (C) by CFU assay. Data expressed as a logarithmic value of the mean number of viable bacteria, and standard deviations indicated with the vertical bars (n= 3-4 mice/ group, ☆$p<0.05$ using the Student's t-test).

The mycobacterial load in the LBP+/+ mice was stable between days 31 and 55, but in the LBP-/- mice, there was significant growth in the liver and lungs (Fig. 3.14A and Fig. 3.14C). There was no significant difference in the spleen CFU between the two groups (Fig. 3.14B).

3.2.5 Analysis of Organ weights of LBP+/+ vs.. LBP-/- mice

During necropsy, the masses of the liver, spleen and lungs were recorded and later expressed as a ratio of the respective mouse body weight (BW). These calculations give an indication of the developing inflammatory response with respect to the cellular recruitment within the organs.

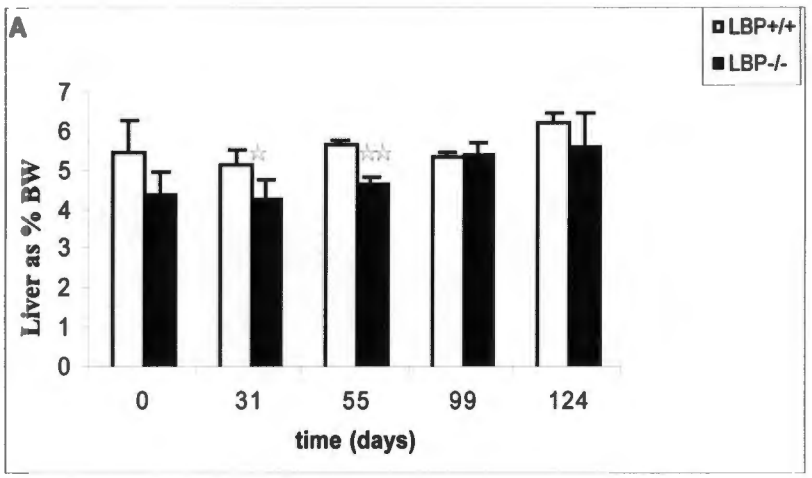

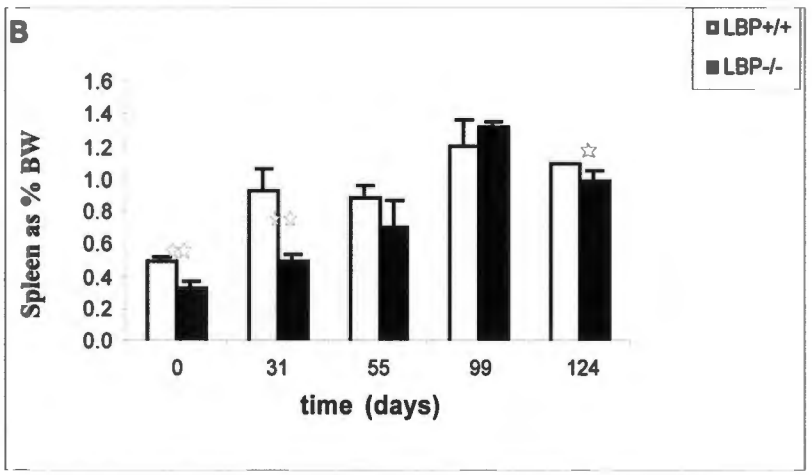

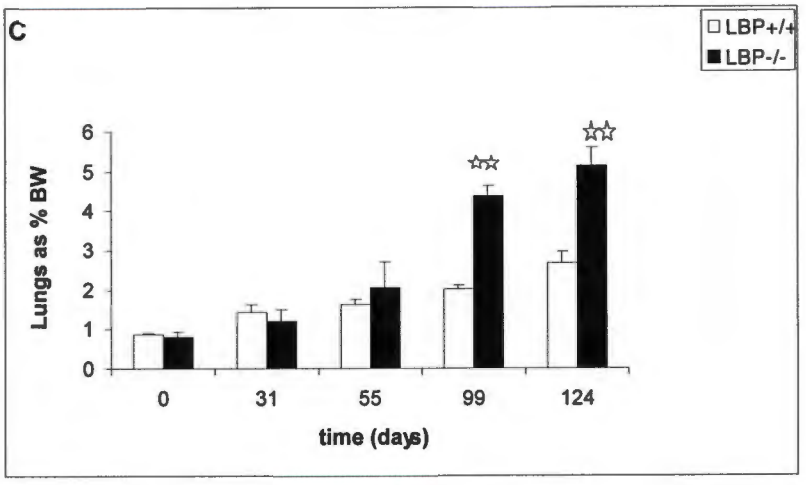

Fig. 3.15: Analysis of organ weights: BW ratio. (A) liver expressed as a ratio of BW, (B) Spleen expressed as a ratio of BW, and (C) Lungs expressed as a ratio of BW (n=3-4 mice/ group☆ $p < 0.05$, ☆☆ $P < 0.01$ using the student t-test)

The most significant difference was observed when comparing the lung: BW ratio of the LBP-/- to those of the LBP +/+ (Fig 3.15C), indicating enhanced inflammation in the C3H/HeJ lungs. This ratio is skewed by the increased LBP-/- weight loss (Fig. 3.13B), but the relevance of the observation is supported by macroscopic evidence (Fig. 3.16). There is no significant difference in the lung: BW ratio of the two groups up to two months, but thereafter, the LBP-/- lungs become massively congested and the ratio is about two-fold greater than the LBP+/+ lungs. The LBP+/+ spleen: BW ratio is initially much larger than the LBP-/- spleen: BW ratio, but as the infection progresses, the spleen: BW ratios become comparable in the two groups (Fig. 3.15B). There is no significant trend in the liver: BW ratio between the two groups (Fig. 3.15A).

3.2.6 Macroscopic Inspection of the Organs of the LBP+/+ vs. LBP-/- mice

The organs were inspected during necropsy and any macroscopic differences noted.

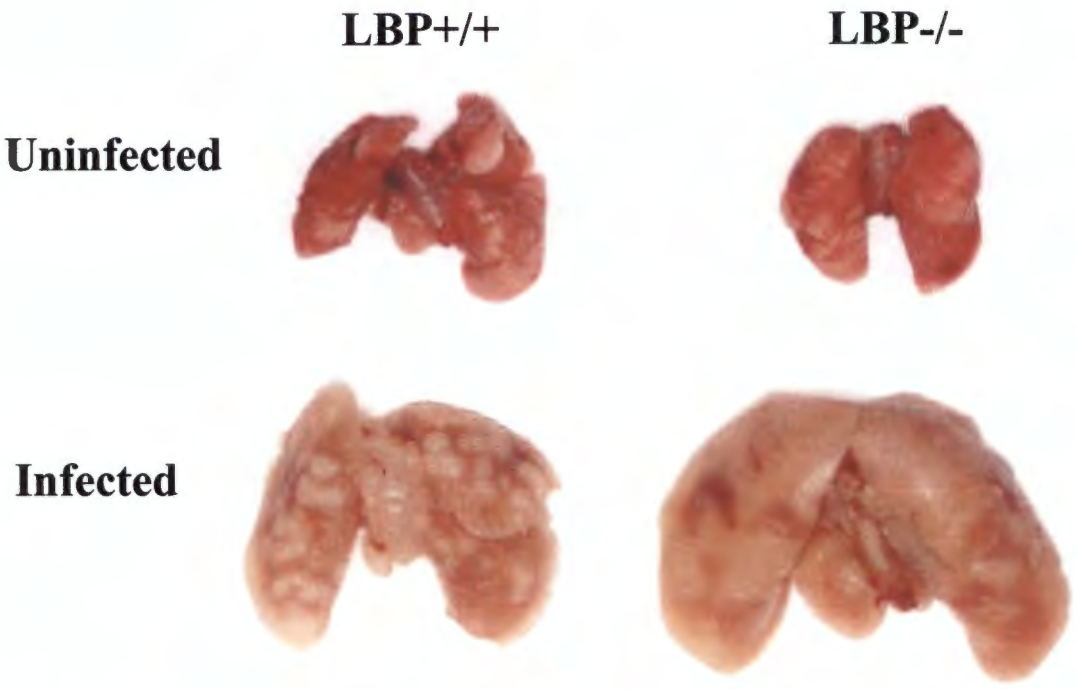

Fig. 3.16: Macroscopic inspection of the lungs of the LBP+/+ vs. LBP-/- mice. Uninfected lungs were taken from naive mice. Infected lungs were taken from mice 14 weeks post-infection (n=3 mice/ group).

The macroscopic analysis indicates that the LBP+/+ lungs are covered with necrotic lesions, whereas these lesions are absent in the LBP-/- lungs. The LBP-/- lungs are significantly larger than the LBP+/+ lungs, indicating a greatly enhanced inflammatory process.

3.2.7 Histological analysis of LBP+/+ vs. LBP-/- mice infected with M.tuberculosis

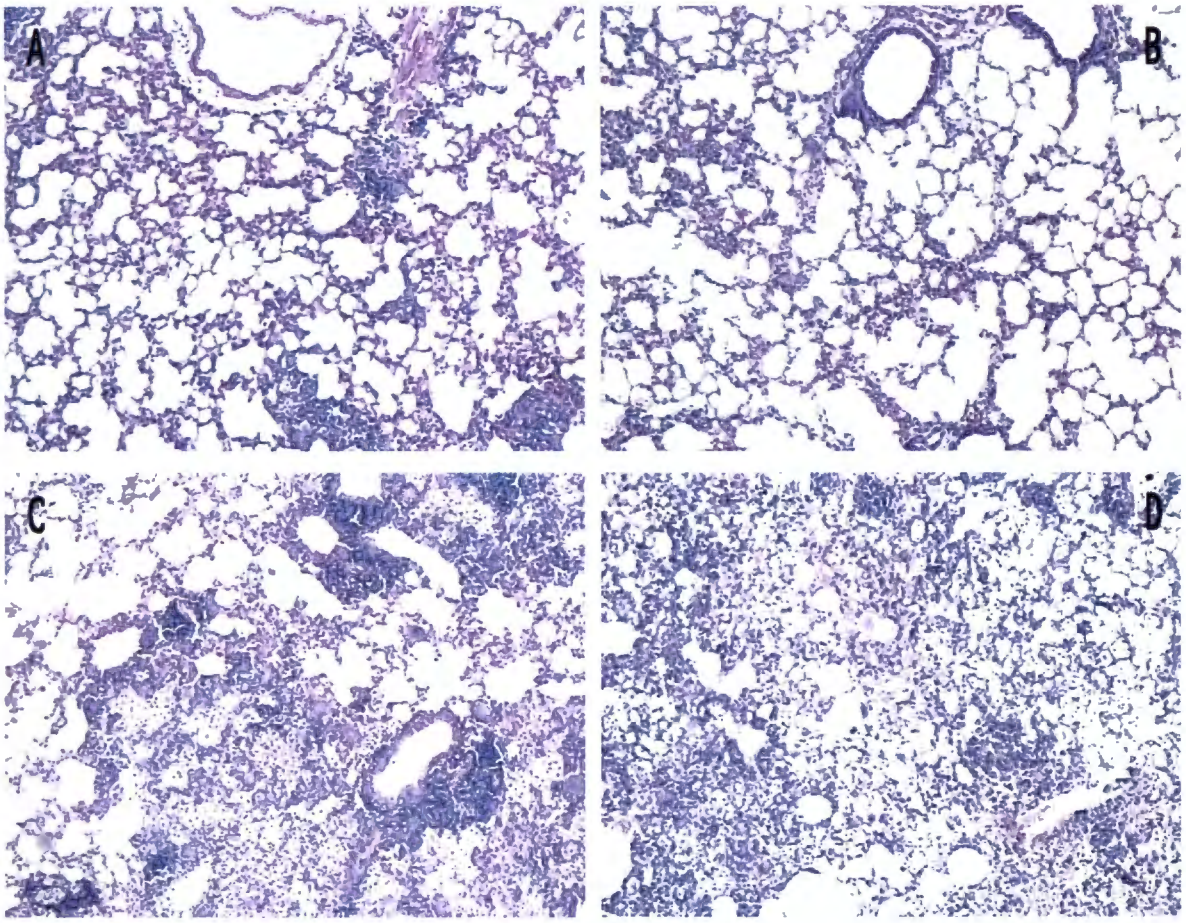

Fig. 3.17: Microscopic alterations in lungs of LBP+/+ (left panels) and LBP-/- mice (right panels) 32 days (A, B) and 55 days (C, D) post aerosol *M.tb* infection using HE stains (histology performed on 2 sections per mouse, 3-4 mice per group)

HE stains of lung sections at 32 days post-infection revealed that there was a comparable level of inflammation in the two groups of mice. Lymphocytic infiltration appeared normal in the two groups of mice. At 55 days however the LBP-/- lungs appeared significantly more congested than the LBP+/+ lungs with increased obstruction of airspace. Large areas of foamy macrophages were seen in lungs from both groups, but appeared to be more prominent in the LBP-/- lungs.

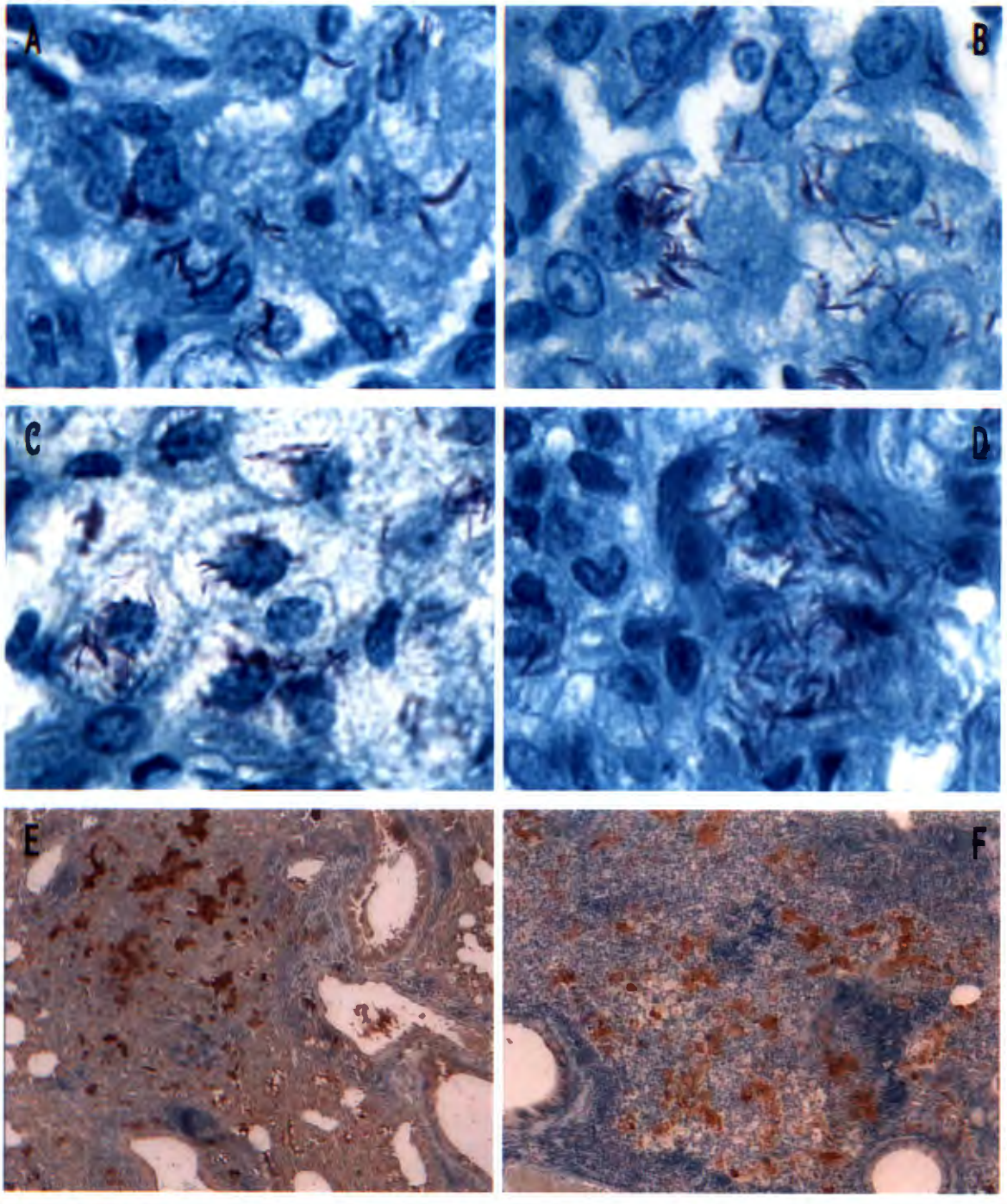

Fig. 3.18: ZN stain for acid-fast bacilli (A-D) and iNOS2 (E,F) in lungs of LBP+/+ (left panels) and LBP-/- mice (right panels) 32 days (A,B), 56 days (C,D) and 56 days (E,F) post aerosol *M.tb* infection (histology performed on 2 sections per mouse, 3–4 mice per group)

The ZN stain revealed that at 32 days post-infection there was a comparable level of AFBs detected in the lungs of both groups of mice (Fig. 3.18A and Fig. 3.18B), and no noticeable difference in AFBs after 55 days (Fig. 3.18C and Fig. 318D). The iNOS2 stain indicated there

was no difference in the expression of iNOS2 between the two groups at 55 days post-infection (Fig. 3.18E and Fig. 3.18F).

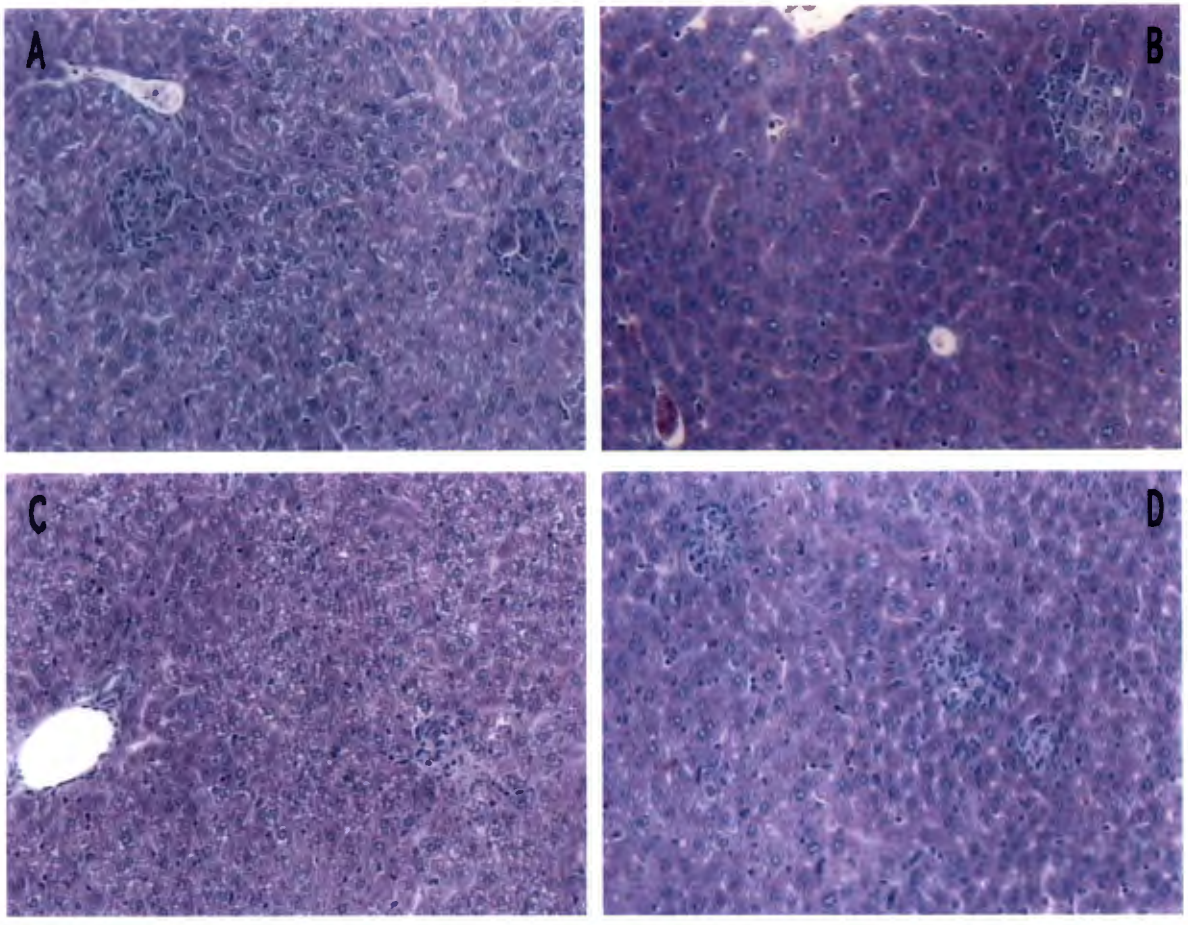

Fig. 3.19: Microscopic alterations in livers of LBP+/+ (left panels) and LBP-/- mice (right panels) 32 days (A,B) and 55 days (C,D) post aerosol *M.tb* infection using HE stains (histology performed on 2 sections per mouse, 3-4 mice per group).

The HE stain in the liver revealed that 32 days post-infection there is a similar inflammatory response in the LBP+/+ and LBP-/- with respect to granulomata development. At 55 days post-infection however, there appears to be an increased granulomatous response in the liver of the LBP-/- when compared to the LBP+/+ liver.

In conclusion, these preliminary data demonstrate that LBP is required for host resistance to *M.tb* infection. Therefore, the two components of the endotoxin response system investigated, TLR4 and LBP, are both required to control infection.

3 Discussion

In this thesis I investigated the *in vivo* role of pattern recognition receptors (PRR) in *M.tb* infection. Recognition of pathogens by PRR leads to activation of antigen presenting cells and induction of a strong innate immune response. Among the PRR, I have focused on the endotoxin receptors, which comprise primarily CD14, LBP and TLR4. As the CD14 KO mouse was unavailable during this study, I investigated the TLR4 mutant and the LBP KO in aerosol *M.tb* infection. In view of the recently published *in vitro* data demonstrating TLR-dependent cellular activation in a CD14 and LBP independent manner, our *in vivo* data is surprising (29)

4.1 The Role of TLR4 in the Induction of Protective Immunity to *Mycobacterium tuberculosis*

Chinese Hamster Ovary (CHO) fibroblast cells transfected with CD14 and TLR2, but not TLR4, acquire the ability to be activated by the mycobacterial cell wall glycolipid lipoarabinomannan (LAM). Subsequently, it was discovered that arabinosylated LAM (AraLAM) derived from rapidly growing mycobacteria could activate the CHO cells in a TLR2 dependent manner, whereas *M.tb* derived mannosylated LAM (ManLAM) could not. In contrast to this, live *M.tb* bacilli mediated cellular activation of the TLR-expressing CHO cells suggesting *M.tb* derived TLR ligands distinct from LAM. Cellular activation mediated by live *M.tb* was demonstrated to occur in a TLR2- and TLR4-dependent manner using TLR-transfected CHO cells and RAW264.7 macrophages. This activation was shown to be independent of LBP or membrane-bound CD14 (29). A heat-labile cell-associated mycobacterial factor was found to activate CHO cells in a TLR4-dependent fashion while a soluble heat-stable mycobacterial factor mediated TLR2–dependent activation. Thus, TLR2 and TLR4 are implicated in the recognition of *M.tb*-derived PAMPs.

Microbial lipoproteins, in particular the 19-kD antigen have been demonstrated *in vitro* to trigger host defence mechanisms in a TLR2-dependent manner (45) Strong induction of macrophage-derived IL-12 and NO were observed in response to this antigen, which was dramatically inhibited by TLR2 neutralising antibodies. The production of TNFα by macrophages has also been shown to be mediated primarily by TLR2 in response to *M.tb*. Induction of TNFα by *M.tb* was demonstrated to be TLR2 specific, as the expression of an

inhibitory TLR2 in a macrophage cell line abrogated this response (46). Furthermore, the expression of TLR2 was sufficient to mediate *M.tb*-induced NF-κB expression in CHO cells. An investigation by Thoma-Uszynski *et al.* demonstrated the induction of direct anti-mycobacterial activity through TLR2. Intracellular replication of *M.tb* within RAW264.7 was dramatically reduced when stimulated with the mycobacterial-derived 19kD lipoprotein (TLR2 ligand) (47). Importantly, TLR2-deficient macrophages did not respond to the 19kD lipoprotein, and displayed no reduction of intracellular growth. This inhibition was shown to be NO-dependent, as blocking the NO pathway with pharmacological inhibitors abrogated the anti-mycobacterial activity induced by the 19kD lipoprotein. In human monocytes and alveolar macrophages, similar anti-mycobacterial activity was induced by the 19kD lipoprotein, however, this was shown to be both NO and TNFα independent (47). In a study by Means *et al*, the LPS antagonist E5531, was demonstrated to dramatically reduce LPS and *M.tb*- induced TNFα production in RAW 264.7 macrophages and primary human alveolar macrophages (48), but did not effect the release of NO. Furthermore, *M.tb* infected peritoneal macrophages from TLR2- and TLR4-deficient mice generated comparable levels of NO to control mice. This investigation implicates TLR4 directly in *M.tb*-induced TNFα production, but suggests a TLR-2 and TLR-4 independent pathway for NO production (48). This is in contrast to the aforementioned study by Thoma-Uszynski *et al,* which demonstrates a role for TLR2 in *M.tb*-induced NO production. The cell wall skeleton *of Mycobacterium bovis bacillus Calmette-Guerin* (BCG-CWS), which consists of peptidoglycan, arabinogalactan and mycolic acids, was shown to induce the maturation of human dendritic cells (49). This BCG-CWS induced maturation was demonstrated to be dependent on autocrine TNFα, as it was inhibited by anti-TNFα mAbs. Furthermore, this TNFα production was TLR-dependent, as TLR-2- and TLR4-deficient macrophages produced significantly less TNFα in response to BCG-CWS (49). This implies that APCs are activated by mycobacterial cell wall antigens in a TLR-dependent manner, and become further activated in an autocrine manner by soluble mediators (such as TNFα). In this study we demonstrate an important function of TLR4 *in vivo* in the induction of protective immunity to *M.tb*.

In this investigation, we assessed the role of TLR4 in *M.tb* infection *in* vivo (approx. 100 bacilli/lung at day 1). The natural mutant C3H/HeJ was used, which has a single-point mutation in the TLR4 gene rendering it dysfunctional (16,17). The C3H/HeJ mice were compared to C3H/HeN mouse, which express the wild-type allele of TLR4. In this study, the C3H/HeJ mice succumbed to the infection between 5 and 7 months, whereas no mortality was observed in the C3H/HeN mice during the duration of the experiment. The body weight

analysis of the mice revealed that the C3H/HeJ mice begin deteriorating from about 5 months post-infection before succumbing. These data demonstrate that TLR4 is an essential PRR in the induction of protective immunity to *M.tb in vivo,* and that other PRRs cannot compensate for its function.

The progression of the infection was monitored by determining the mycobacterial load (CFU analysis) in the liver, spleen and lungs. The pulmonary infection in the two groups progressed at a comparable rate up to 1 month, thereafter a significant difference was observed. Two months into the infection, the C3H/HeN mice effectively controlled the growth of the bacilli. In contrast, the C3H/HeJ mice were not able to suppress the infection, and at 5 months post-infection the bacterial load was one log greater than that observed in C3H/HeN lungs. This trend was also observed systemically in the liver and spleen a month post-infection. Insignificant growth was observed in the liver and spleen of the C3H/HeN mice. Increased growth was observed in the liver of the mutants, Specifically, a one log higher CFU in the liver, and almost two logs greater in the spleen. Interestingly, there is no further bacterial growth in the C3H/HeJ lung between 13 and 20 weeks, which might indicate a delayed mycobacteriastatic mechanism in the mutant lung

During necropsy, organs were removed, observed macroscopically, weighed and expressed as a ratio of the mouse's body weight. No significant difference was observed in the liver or lung ratio when comparing the two groups, thus indicating a normal level of inflammation in these organs. The increased splenomegaly observed in the C3H/HeJ mouse indicates that significantly increased cellular recruitment within this organ is associated with an increased bacterial burden.

Development of the inflammatory response within the lung was found to be to be comparable in the two groups. Lung granulomata appear fully developed at 1 month, but there is a less pronounced lymphocytic presence in the C3H/HeJ lungs concomitant with an increased neutrophil component. This could indicate that macrophages present in the lung are unable to contain the infection, and as a compensatory mechanism, neutrophils are recruited to assist with the killing. Foamy macrophages appear at this stage of the infection, but become more prevalent as the infection develops. The number of hepatic granulomata and cellular composition is comparable at this stage, comprising a few diffuse structures. The quantity of acid-fast bacilli (AFBs) appears similar up to 2 months in the lungs. At 5 months post-infection, AFBs were not readily detected in the C3H/HeN lungs, but were abundant in the

lungs of the mutants. This observation correlates with the CFU determination in the lungs. As the infection progresses, a greater inflammatory response is seen in the liver of the C3H/HeJ mice (approx. 5-fold more granulomata at 5 months) which corresponds with the greater CFU in the mutant liver. Surprisingly, immunohistochemistry (IHC) analysis revealed that the expression of the enzyme inducible nitric oxide synthase-2 (iNOS2) was comparable at 2 and 5 months post-infection. This would indicate that the C3H/HeJ macrophages are in an activated state, and can generate RNI to mediate killing of bacilli. This finding might explain the apparent resistance observed in the lungs of the C3H/HeJ mice from 13 to 20 weeks, where no further increase in CFU is seen. To clarify this situation, IHC for iNOS2 should be performed at an earlier time point to determine whether this mechanism is delayed. Evidence from the literature however tends to support the above proposition. Specifically, i*n vitro* RNI production is purportedly induced by the synergistic action of IFNγ and TNFα (43). Greenberg et al. reported that *in vivo* intratracheal administration of heat-killed *M.tb* resulted in rat alveolar macrophage-derived iNOS-2 mRNA expression and RNI independent of TNFα production (50). This is further substantiated by the study of Means *et al.* (48), in which a TLR-2 and TLR–4 independent mechanism for M.tb-induced NO was indicated. These studies therefore support our finding of similar iNOS-2 expression in the lungs despite a significant difference in TNFα levels.

Bronchoalveolar lavage (BAL) was performed at 4 weeks post-infection to investigate the nature of the cellular recruitment. No neutrophils were seen in the BALs taken from the C3H/HeN mice, but a significant level was observed in the BALs from the C3H/HeJ mice. The continuing neutrophil recruitment might be a compensatory mechanism deployed by the mutant to control the infection, albeit unsuccessfully. A neutrophil response has been shown to be effective against fast growing bacilli, but has been proposed to be relatively ineffective in retarding the replication of slow replicating bacilli such as *M.tb* (51). A significant decrease in the proportion of macrophages was also observed in the BAL samples taken from the C3H/HeJ mice, which would also effect their ability to contain the infection. The lymphocyte composition in the BAL fluid was comparable in the two groups.

To assess the level of pro-inflammatory cytokines, BAL fluid and lung homogenates were analysed for the presence of IL-12p40, IFNγ, TNFα and the chemokine MCP-1. The production of IL-12p40, a component of the cytokine, IL-12 which promotes the emergence of T_H1, IFNγ-producing T cells (4), was shown to be significantly lower in both the BAL fluid and the lung homogenate of the C3H/HeJ mouse. This reduced level of IL-12p40 might be a

consequence of reduced macrophage induction due to defective TLR4 expression. A similar decrease in IL-12 production by C3H/HeJ peritoneal macrophages was recently noted in response to an array of Gram-negative and –positive microorganisms tested (52). The significance of IL-12 in the protective immune response to *M.tb* has been demonstrated with anti-IL-12 neutralising antibodies, which resulted in impaired resistance, diffuse hepatic granulomata and a reduction in total mononuclear cell accumulation (53). In humans deficient in the IL-12 receptor (IL-12R), an impairment of mycobacterial immunity is seen concomitant with a decrease in IFNγ production by activated NK cells and T cells (54). Furthermore, mice deficient for IL-12p40, display dramatically reduced protective immunity to *M.tb,* and succumb to the infection (38). IFNγ is absolutely required for the activation of macrophages and the subsequent development of granuloma during a *M.tb* infection (55). IFNγ-deficient mice are highly susceptible to *M.tb,* and succumb rapidly to infection. (35). A decrease in IFNγ production was observed in the BAL fluid (data not shown) and lung homogenates of the C3H/HeJ mice as a consequence of reduced APC-derived IL-12, but not at a significantly lower level. TNFα secretion during mycobacterial infection has been shown to mediate essential functions including the upregulation of vascular adhesion molecules (5) and the recruitment of mononuclear cells for the formation of granuloma (39,40). TNFα was produced comparably in the BAL fluid, but was significantly lower in the lung homogenates of the C3H/HeJ mice. This finding of decreased TNFα is supported by the studies of Tsuji et al (49) and Means et al (48), which demonstrate a role for TLR2 and TLR4 in mycobacteria-induced TNFα production. This difference in TNFα secretion can be a result of (i) a lower proportion of TNFα-secreting macrophages observed in the BAL fluid and/or (ii) impaired macrophage function/activation. Taken together the cytokine analysis corroborates our findings of increased susceptibility of C3H/HeJ mice at the systemic level.

The chemokine MCP-1, released predominantly by macrophages, attracts T lymphocytes and monocytes, which are primary components of the granulomatous response (41). Studies addressing the role of MCP-1 in *M.tb* infection have been controversial. Mice treated with anti-MCP-1 antibodies had normal granuloma formation when exposed to beads coupled to purified protein derivative (PPD) of *M.tb* (56). Surprisingly, MCP-1-deficient mice were indistinguishable from wild-type mice in their ability to clear an intravenous infection with M.tb (57), but aerosol challenge might yield different results. However, MCP-1 levels in patient's BAL fluid increase with a pulmonary tuberculosis infection, and decline during recovery, confirming an association between active tuberculosis with enhanced MCP-1 production (42). No MCP-1 was detected in the BAL fluid of C3H/HeN or C3H/HeH mice,

but was measurable in the lung homogenates at 4 weeks post-infection. This might indicate that MCP-1 is present in the interstitium at this time point, but not in the alveolar spaces. The level of MCP-1 was significantly higher in the C3H/HeN lungs, which could account partly for the reduced macrophage population in the BAL fluid of the C3H/HeJ mice.

In conclusion, we have shown TLR4 appears an essential component of protective immunity to *M.tb*. This PRR has systemic effects on mortality, control of bacterial burden, dissemination of infection, control of pro-inflammatory cytokines, and cellular recruitment. Further investigation is required to gain insight into the susceptibility of the C3H/HeJ mouse, namely:

(i) INOS2 IHC performed at earlier time points

(ii) chemokine level analysis in the lungs to explain the differences observed in cellular recruitment.

4.2 The Role of LBP in the Induction of Protective Immunity to *M.tuberculosis*

It has been demonstrated that serum concentrations of LPS-activity modulating proteins, LBP and sCD14 are elevated in patients with active tuberculosis (58). During convalescence or treatment, the levels of these proteins declines suggesting they mediate a protective role. *M.tb* uptake by human microglial cells has been shown to be inhibited significantly by the addition of anti-CD14 antibodies or sCD14. This activity was enhanced by the addition of LBP, which suggests that it facilitates *M.tb*-CD14 interactions, an analogous role mediated by LBP in the LPS response (33). Heat-killed Gram-positive bacteria activated CHO and HEK293 cells transfected with TLR2, but not TLR4 (59,60). Yoshimura *et al.* demonstrated that co-expression of CD14 with TLR2 in CHO cells significantly enhanced NF-κB translocation after exposure to heat-killed *S.aureus*. This data suggests that CD14 may act as a co-receptor for TLR proteins, enhancing the sensitivity of macrophages and neutrophils to pathogens (58). Furthermore, mycobacteria-induced NF-κB activation was enhanced by co-expressing CD14 (34). In contrast to this, TLR-2 and TLR-4 expressing CHO cells mediate cellular activation by *M.tb* in a CD14 and LBP independent manner (29). These discrepancies reported for CD14 and LBP might reflect species-specific differences in TLR recognition or subtle flaws in the experimental design of the in vitro studies (61). Given the above observations and our findings regarding TLR4, we investigated the role of LBP in in *vivo M.tb* infection.

LBP+/+ mice survived the duration of the experiment (approx. 100 bacilli/lungs at day 1), but LBP-/- mice succumbed to the infection between 9 and 19 weeks. Body weight analysis indicated that LBP-/- mice begin deteriorating at 11 weeks and succumb steadily thereafter.
To investigate the development of the infection, the mycobacterial load in the liver, spleen and lungs were assessed. The CFU in these organs were comparable 31 days post-infection, but significantly increased growth in the LBP-/- liver was determined 55 days post-infection when compared to the LBP+/+ mice. The pulmonary infection appeared to be suppressed in the LBP+/+ mice at day 51, but increased significantly in the LBP-/- lungs. The spleen CFU was comparable in the two groups. This demonstrates that the liver and lungs of LBP-/- mice have difficulty in controlling the *M.tb* infection. LBP+/+ spleen ratio to body weight (BW) was initially larger than the LBP-/- spleen to BW ratio, but as the infection progressed, the LBP-/- spleen to BW ratio became comparable. A highly significant increase in the size of the LBP-/- lungs was observed 99 days post-infection (ratio to BW is about two-fold greater than the LBP+/+). Macroscopically, after 99 days, the LBP+/+ lungs appear severely necrotic with lesions covering the organ. In contrast, the LBP-/- lungs are massive compared to the LBP+/+ lungs, but have no necrotic lesions. This demonstrates that chronic pulmonary *M.tb* in LBP+/+ mice results in a hyperactive immune response leading to lung tissue necrosis. The LBP-/- mice, which have a more severe infection, appear to mount hyporesponsive immunity. This inability to control the infection in the LBP-/- mice leads to exacerbated cellular recruitment into the lungs, congestion and death. This data is supported by the histological analysis, which reveals a dramatic increase in cellular infiltration in the mutant lungs at day 99 and obstruction of air spaces. There were no difference in the ability to generate NO in the lungs at the time point analysed (as assessed by iNOS2 reactivity at day 32) between the two groups of mice. In conclusion, preliminary data from this study reveals a role for LBP in *M.tb* infection. LBP has systemic effects on mortality, control of bacterial burden and dissemination of infection. Further investigation is required to gain insight into the susceptibility of the LBP-/- mice, namely:

(i) The levels of pro-inflammatory cytokines produced, such as IL-12, IFNγ and TNFα.

(ii) The nature of cellular recruitment into the lungs.

(iii) An extended CFU study performed to observe the progression of pulmonary infection.

However, it should be noted that the results with the LBP-/- mice and *M.tb* are preliminary and should be subjected to careful analysis. The LBP-/- mice are on a mixed genetic background (BALB/c x 129sv), whereas the control mice used are on a pure BALB/c background. This obscures the analysis as the LBP-/- mice have a mixed MHC haplotype (H-2^{dxb}) and the wild-type mice have an H-2^{d} haplotype. The difference in MHC molecules would result in different peptide affinities, peptide presentation and an altered response. Furthermore, the difference in genetic backgrounds might lead to a variation in host resistance or susceptibility genes, which may further confuse the analysis. I would speculate that the significant differences observed cannot be merely attributed to the genetic backgrounds, but these results must be confirmed with appropriate controls.

4.3 Summary

In this investigation we demonstrate a role for the endotoxin receptors TLR4 and LBP in the induction of protective immunity to pulmonary *M.tb* infection. TLR4 is an essential pattern recognition receptor for the early detection of a *M.tb* infection in the host and the subsequent triggering of the innate immune response. In the absence of TLR4, C3H/HeJ mice display increased susceptibility to *M.tb* infection and succumb to the infection.

Preliminary studies with LBP indicate that it is an essential component of this mycobacterial recognition system. We propose the following mechanism: After infection with *M.tb*, LBP facilitates the transfer of *M.tb*-derived PAMPs (yet to be identified) to the surface of APCs, where they engage the 'LPS' receptor complex CD14/TLR4 (refer to the figure below). Signalling events take place leading to NFκB activation and subsequent transcription of pro-inflammatory genes.

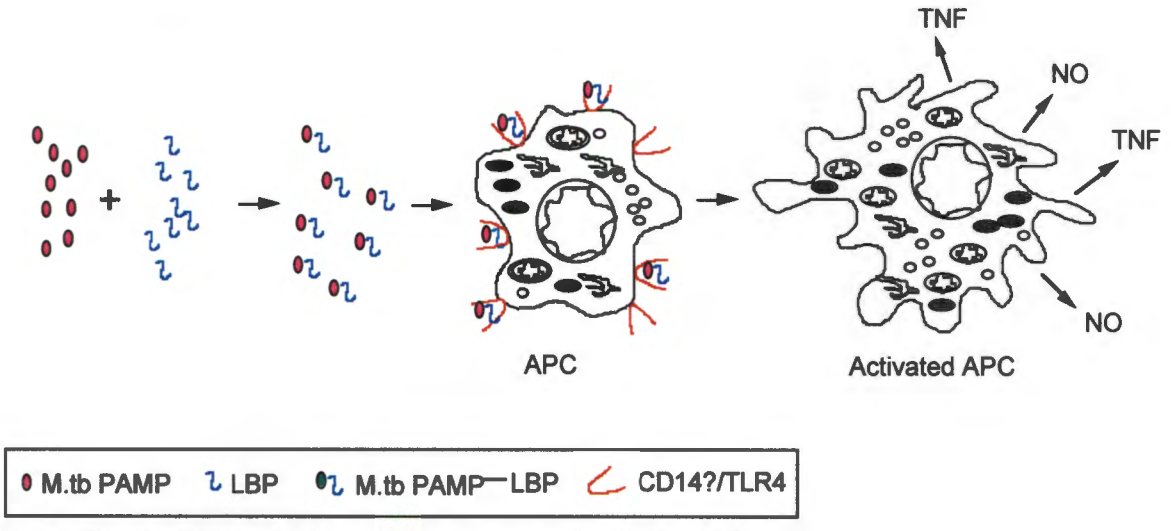

Fig. 1.4: Hypothetical mechanism of macrophage activation by *M.tb*

***M.tuberculosis*-derived PAMPs (*M.tb*-PAMPs) are transferred to the surface of antigen-presenting cells by LBP, where interaction with TLR-2 or -4 occurs. The role of CD14 in mycobacterial recognition and APC activation has yet to be defined.**

5. References

1. **Flynn, J. L., and J. D. Ernst.** Opin Immunol 2000 Aug. Immune responses in tuberculosis *Curr 12:432.*

2. **Bloom, B. R., and C. J. Murray.** 1992. Tuberculosis: commentary on a reemergent killer. *Science 257:1055.*

3. **Goren, M. B., D. A. H. P, M. R. Young, and J. A. Armstrong.** 1976. Prevention of phagosome-lysosome fusion in cultured macrophages by sulfatides of Mycobacterium tuberculosis. *Proc Natl Acad Sci U S A 73:2510.*

4. **Trinchieri, G.** 1995. Interleukin-12: a proinflammatory cytokine with immunoregulatory functions that bridge innate resistance and antigen-specific adaptive immunity. *Annu Rev Immunol 13:251.*

5. **Weill, D., Wautier J.L., Dosquet C, Wautier M.P., Carreno M.P., Boval B.** 1995. Monocyte modulation of endothelial leukocyte adhesion molecules. J Lab Clin Med. 125: 768

6. **Blanden, R. V., M. J. Lefford, and G. B. Mackaness.** 1969. The host response to Calmette-Guerin bacillus infection in mice. *J Exp Med 129:1079.*

7. **McDonough, K. A., Y. Kress, and B. R. Bloom.** 1993. Pathogenesis of tuberculosis: interaction of Mycobacterium tuberculosis with macrophages [published erratum appears in Infect Immun 1993 Sep;61(9):4021-4]. *Infect Immun 61:2763.*

8. **Flynn, J. L., M. M. Goldstein, K. J. Triebold, B. Koller, and B. R. Bloom.** 1992. Major histocompatibility complex class I-restricted T cells are required for resistance to Mycobacterium tuberculosis infection. *Proc Natl Acad Sci U S A 89:12013.*

9. **Fearon, D. T., and R. M. Locksley.** 1996. The instructive role of innate immunity in the acquired immune response. *Science 272:50.*

10. **Janeway, C. A., Jr.** 1989. Approaching the asymptote? Evolution and revolution in immunology. *Cold Spring Harb Symp Quant Biol 54 Pt 1:1.*

11. **Hashimoto C, Hudson K.L., and Anderson K.V.** 1998. The Toll gene of Drosophila, required for the dorso-ventral embryonic polarity, appears to encode a transmembrane protein. Cell 52:269.

12. **Lemaitre B, Nicolas E, Michaut L, Reichart J.M. and Hoffmann J.A.** 1996. The dorsoventral regulatory gene cassette spatzle/Toll/cactus controls the potent antifungal response in Drosophila adults. Cell 86:973.

13. **Medzhitov, R., P. Preston-Hurlburt, and C. A. Janeway, Jr.** 1997. A human homologue of the Drosophila Toll protein signals activation of adaptive immunity [see comments]. *Nature 388:394.*

14. **Pugin, J., I. D. Heumann, A. Tomasz, V. V. Kravchenko, Y. Akamatsu, M. Nishijima, M. P. Glauser, P. S. Tobias, and R. J. Ulevitch.** 1994. CD14 is a pattern recognition receptor. *Immunity 1:509.*

15. **Ulevitch, R. J., and P. S. Tobias.** 1995. Receptor-dependent mechanisms of cell stimulation by bacterial endotoxin. *Annu Rev Immunol 13:437.*

16. **Poltorak, A., X. He, I. Smirnova, M. Y. Liu, C. V. Huffel, X. Du, D. Birdwell, E. Alejos, M. Silva, C. Galanos, M. Freudenberg, P. Ricciardi-Castagnoli, B. Layton, and B. Beutler.** 1998. Defective LPS signaling in C3H/HeJ and C57BL/10ScCr mice: mutations in Tlr4 gene. *Science 282:2085.*

17. **Qureshi, S. T., L. Lariviere, G. Leveque, S. Clermont, K. J. Moore, P. Gros, and D. Malo.** 1999. Endotoxin-tolerant mice have mutations in Toll-like receptor 4 (Tlr4) [see comments] [published erratum appears in J Exp Med 1999 May 3;189(9):following 1518]. *J Exp Med 189:615.*

18. **Peterson, P. K., G. Gekker, S. Hu, W. S. Sheng, W. R. Anderson, R. J. Ulevitch, P. S. Tobias, K. V. Gustafson, T. W. Molitor, and C. C. Chao.** 1995. CD14 receptor-mediated uptake of nonopsonized Mycobacterium tuberculosis by human microglia. *Infect Immun 63:1598.*

19. **Savedra, R., Jr., R. L. Delude, R. R. Ingalls, M. J. Fenton, and D. T. Golenbock.** 1996. Mycobacterial lipoarabinomannan recognition requires a receptor that shares components of the endotoxin signaling system. *J Immunol 157:2549.*

20. **Ingalls, R. R., B. G. Monks, R. Savedra, Jr., W. J. Christ, R. L. Delude, A. E. Medvedev, T. Espevik, and D. T. Golenbock.** 1998. CD11/CD18 and CD14 share a common lipid A signaling pathway. *J Immunol 161:5413.*

21. **Jack, R. S., X. Fan, M. Bernheiden, G. Rune, M. Ehlers, A. Weber, G. Kirsch, R. Mentel, B. Furll, M. Freudenberg, G. Schmitz, F. Stelter, and C. Schutt.** 1997. Lipopolysaccharide-binding protein is required to combat a murine Gram- negative bacterial infection. *Nature 389:742.*

22. **Haziot, A., E. Ferrero, F. Kontgen, N. Hijiya, S. Yamamoto, J. Silver, C. L. Stewart, and S. M. Goyert.** 1996. Resistance to endotoxin shock and reduced dissemination of Gram- negative bacteria in CD14-deficient mice. *Immunity 4:407.*

23. **Hoshino, K., O. Takeuchi, T. Kawai, H. Sanjo, T. Ogawa, Y. Takeda, K. Takeda, and S. Akira.** 1999. Cutting edge: Toll-like receptor 4 (TLR4)-deficient mice are hyporesponsive to lipopolysaccharide: evidence for TLR4 as the Lps gene product. *J Immunol 162:3749.*

24 **Wright S.D., Ramos R.A., Tobias P.S., Ulevitch R.J. and Mathison J.C.** 1990. CD14, a receptor for complexes of lipopolysaccharide (LPS) and LPS binding protein. Science. 249:1431.

25. **Glode, L. M., I. Scher, B. Osborne, and D. L. Rosenstreich.** 1976. Cellular mechanism of endotoxin unresponsiveness in C3H/HeJ mice. *J Immunol 116:454.*

26. **Watson, J., and R. Riblet.** 1975. Genetic control of responses to bacterial lipopolysaccharides in mice. II. A gene that influences a membrane component involved in the activation of bone marrow-derived lymphocytes by lipipolysaccharides. *J Immunol 114:1462.*

27. **AD, O. B., D. L. Rosenstreich, and B. A. Taylor.** 1980. Control of natural resistance to Salmonella typhimurium and Leishmania donovani in mice by closely linked but distinct genetic loci. *Nature 287:440.*

28. **Takeuchi, O., K. Hoshino, T. Kawai, H. Sanjo, H. Takada, T. Ogawa, K. Takeda, and S. Akira.** 1999. Differential roles of TLR2 and TLR4 in recognition of Gram-negative and Gram-positive bacterial cell wall components. *Immunity 11:443.*

29. **Means, T. K., S. Wang, E. Lien, A. Yoshimura, D. T. Golenbock, and M. J. Fenton.** 1999. Human toll-like receptors mediate cellular activation by Mycobacterium tuberculosis. *J Immunol 163:3920.*

30. **Ramadori, G., K. H. Meyer zum Buschenfelde, P. S. Tobias, J. C. Mathison, and R. J. Ulevitch.** 1990. Biosynthesis of lipopolysaccharide-binding protein in rabbit hepatocytes. *Pathobiology 58:89.*

31. **Grube, B. J., C. G. Cochane, R. D. Ye, C. E. Green, M. E. McPhail, R. J. Ulevitch, and P. S. Tobias.** 1994. Lipopolysaccharide binding protein expression in primary human hepatocytes and HepG2 hepatoma cells. *J Biol Chem 269:8477.*

32. **Schumann, R. R.** 1992. Function of lipopolysaccharide (LPS)-binding protein (LBP) and CD14, the receptor for LPS/LBP complexes: a short review. *Res Immunol 143:11.*

33. **Peterson, P. K., G. Gekker, S. Hu, W. S. Sheng, W. R. Anderson, R. J. Ulevitch, P. S. Tobias, K. V. Gustafson, T. W. Molitor, and C. C. Chao.** 1995. CD14 receptor-mediated uptake of nonopsonized Mycobacterium tuberculosis by human microglia. *Infect Immun 63:1598.*

34. **Portnoy, D. A., Schreiber, R. D., Connely, P., Tilney, L. G.** 1989. Gamma interferon limits access of listeria monocytogenes into the cytoplasm. J. Exp. Med. 170: 2141

35. **Dalton, D. K., Pitts-Meek S, Figari I. S., Bradley, A, Stewart T. A.** 1993. Multiple defects of immune cell function in mice with disrupted interferon-gamma genes. Science. 259: 1739.

36. **Kobayashi, M., Fitz, L., Ryan, M., Hewick, R.M., Clark, S.C., Chan, S., Loudon, R., Sherman, F., Perussia, B. and G., T.** 1989. Identification and purification of natural killer cecll stimulatory factor (NKSF), a cytokine with multiple biological effects on human lymphocytes. J. Exp. Med. 170: 827.

37. **Ma, X., Chow, J. M., Gri, G., Carra, G., Gerosa, F., Wolf, S. F., Dzialo, R, and Trinchieri, G.** 1996. The interleukin 12p40 gene promotor is primed by interferon gamma in monocytic cells. J. Exp. Med. 183: 147.

38. 52. **Cooper, A. M., J. Magram, J. Ferrante, and I. M. Orme.** 1997. Interleukin 12 (IL-12) is crucial to the development of protective immunity in mice intravenously infected with mycobacterium tuberculosis. *J Exp Med 186:39.*

39. **Jacobs, M, Marino, M. W., Brown, N. Abel, B Bekker L. G., Quesniaux V. J., Fick L, Ryffel B.** 2000. Correction of defective host response to Mycobacterium bovis BCG infection in TNF-deficient mice by bone marrow transplantation. Lab. Invest. 80: 901

40. **Bean A. G., Roach, D. R., Briscoe, H, France, M. P., Korner, H, Sedgewick, J. D., Britton, W. J.** 1999. Structural deficiencies in granuloma formation in TNF gene-targeted mice underlie the heightened susceptibility to aerosol Mycobacterium tuberculosis infection, which is not compensated for by lymphotoxin. J. Immunol. 162: 3504.

41. **Taub, D. D., Proost, P, Murphy, W. J., Anver, M, Longo, D. L., van Dammer, J, Oppenheim, J. J.** 1995. Monocyte chemotactic protein-1 (MCP-1), -2, and –3 are chemotactic for human T lymphocytes. J. Clin. Invest. 95: 1370.

42. **Kurashima, K, Mukaida, N, Fujimura, M, Yasui, M, Nakazumi, Y, Matsuda, T, Matsushima, K.** 1997. Elevated chemokine levels in bronchoalveolar lavage fluid of tuberculosis patients. Am. J. Respir. Crit. Care. Med. 155: 1474.

43. **Xie, Q. W., R. Whisnant, and C. Nathan.** 1993. Promoter of the mouse gene encoding calcium-independent nitric oxide synthase confers inducibility by interferon gamma and bacterial lipopolysaccharide. *J Exp Med 177:1779.*

44. **MacMicking, J. D., North R. J., LaCourse R., Mudgett J. S., Shah, S. K., Nathan C. F.** 1997. Identification of nitric oxide synthase as a protective locus against tuberculosis. Proc. Natl. Acad. Sci. USA. 94: 5243.

45. **Brightbill, H. D, D. H. Libraty, S. R. Krutzik, R. B. Yang, J. T. Belisle, J. R. Bleharski, M. Maitland, M. V. Norgard, S. E. Plevy, S. T. Smale, P. J. Brennan, B. R. Bloom, P. J. Godowski, and R. L. Modlin.** 1999. Host defense mechanisms triggered by microbial lipoproteins through toll-like receptors. *Science 285:732.*

46. **Underhill, D. M., A. Ozinsky, K. D. Smith, and A. Aderem.** 1999. Toll-like receptor-2 mediates mycobacteria-induced proinflammatory signaling in macrophages. *Proc Natl Acad Sci U S A 96:14459.*

47. **Thoma-Uszynski S, Stenger S, Takeuchi O, Ochoa M.T, Engele M, Sieling P.A, Barnes P.F, Rollinghoff M, Bolcskei P.L, Wagner M, Akira S, Norgard M.V, Belisle J.T, Godowski P.J, Bloom B.R, Modlin R.L.** 2001. Induction of Direct Antimicrobial Activity Through Mammalian Toll-like Receptors. Science. 291:1544.

48. **Means T.K, Jones B.W., Schromm A.B., Shurtleff B.A., Smith J.A., Keane J, Golenbock D.T., Vogel S.N. and Fenton M.J.** 2001. Differential Effects of a Toll-like Receptor Antagonist on Mycobacterium tuberculosis-Induced Macrophage Responses. J.Immunol. 166:4074.

49. **Tsuji S, Matsumoto M, Takeuchi O, Akira S, Azuma I, Hayashi A, Toyoshima K, Seya T.** 2000. Maturation of human dendritic cells by cell wall skeleton of Mycobacterium bovis bacillus Calmette-Guerin: involvement of toll-like receptors. Infect. Immun.. 68:6883.

50. **Greenberg, S. S., J. Xie, J. Kolls, C. Mason, and P. Didier.** 1995. Rapid induction of mRNA for nitric oxide synthase II in rat alveolar macrophages by intratracheal administration of Mycobacterium tuberculosis and Mycobacterium avium. *Proc Soc Exp Biol Med 209:46.*

51. **Seiler, P., P. Aichele, B. Raupach, B. Odermatt, U. Steinhoff, and S. H. Kaufmann.** Infect Dis 2000 Feb. Rapid neutrophil response controls fast-replicating intracellular bacteria but not slow-replicating Mycobacterium tuberculosis. *J 181:671.*

52. **Hou, L., H. Sasaki, and P. Stashenko.** Immun 2000 Aug. Toll-like receptor 4-deficient mice have reduced bone destruction following mixed anaerobic infection. *Infect 68:4681.*

53. **Cooper, A. M., Roberts, A. D., Rhoades, E. R., Callahan, J. E., Getzy, D. M. and Orme, I. M.** 1995. The role of interleukin-12 in acquired immunity to Mycobacterium tuberculosis infection. Immunology. 84: 423.

54. **Altare, F., A. Durandy, D. Lammas, J. F. Emile, S. Lamhamedi, F. Le Deist, P. Drysdale, E. Jouanguy, R. Doffinger, F. Bernaudin, O. Jeppsson, J. A. Gollob, E. Meinl, A. W. Segal, A. Fischer, D. Kumararatne, and J. L. Casanova.** 1998. Impairment of mycobacterial immunity in human interleukin-12 receptor deficiency. *Science 280:1432.*

55. **Sugawara I, Yamada H, Kazumi Y, Doi N, Otomo K, Aoki T, Mizuno S, Udagawa T, Tugawa Y and Iwakura Y.** 1998. Induction of granulomas in interferon-gamma gene-disrupted mice by avirulent but not by virulent strains of Mycobacterium tuberculosis. J. Med. Microbiol. 47:871.

56. **Chensue, S. W., K. S. Warmington, J. H. Ruth, P. S. Sanghi, P. Lincoln, and S. L. Kunkel.** 1996. Role of monocyte chemoattractant protein-1 (MCP-1) in Th1 (mycobacterial) and Th2 (schistosomal) antigen-induced granuloma formation: relationship to local inflammation, Th cell expression, and IL-12 production. *J Immunol 157:4602.*

57. **Lu, B. Rutledge, B. J. Gu, L. Fiorilla, J. Lukacs, N. W. Kunkel, S. L. North, R. Gerard, C. Rollins, B. J.** 1998. Abnormalities in monocyte recruitment and cytokine expression in monocyte chemoattractant protein 1-deficient mice. J. Exp. Med. 187: 601.

58. **Juffermans, N. P., A. Verbon, S. J. van Deventer, W. A. Buurman, H. van Deutekom, P. Speelman, and T. van der Poll.** 1998. Serum concentrations of lipopolysaccharide activity-modulating proteins during tuberculosis. *J Infect Dis 178:1839.*

59. **Yoshimura, A., E. Lien, R. R. Ingalls, E. Tuomanen, R. Dziarski, and D. Golenbock.** 1999. Cutting edge: recognition of Gram-positive bacterial cell wall components by the innate immune system occurs via Toll-like receptor 2. *J Immunol 163:1.*

60. **Schwandner, R., R. Dziarski, H. Wesche, M. Rothe, and C. J. Kirschning.** 1999. Peptidoglycan- and lipoteichoic acid-induced cell activation is mediated by toll-like receptor 2. *J Biol Chem 274:17406.*

61. **Medzhitov, R., and C. Janeway, Jr.** Engl J Med 2000 Aug 3. Innate immunity. *N 343:338.*

6. Appendices

ABBREVIATIONS:

AFB	acid-fast bacilli
$^{-/-}$ mice	mice homozygous deficient for specified gene
BW	body weight
dd	double-distilled
DNA	deoxyribonucleic acid
DNTP	deoxyribonucleoside triphosphate
EDTA	ethylenediaminetetraacetic acid
ELISA	enzyme-linked immunosorbent assay
ES cells	embryonic stem cells
EtBr	ethidium bromide
H_2O	water
IFNγ	interferon gamma
IL	interleukin
INOS	inducible nitric oxide synthase
i.p	intraperitoneal
i.v	intravenous
Kb	kilo-bases, length measurement of DNA
KD	kilo Dalton
KO	'knockout', genetically deficient
LCs	lymphocytes
LPS	lipopolysaccharide
M	molar
MCs	macrophages
MCP-1	macrophage chemotactic protein 1
MHC	major histocompatibility complex
Mins	minutes
NK cells	natural killer cells
NO	nitric oxide
NTs	neutrophils
o/n	over night
PBS	phosphate buffered saline

PCR	polymerase chain reaction
RNI	reactive nitrogen intermediate
RO	retro-orbital
Secs	seconds
SPF	specific pathogen free
T_H	T-helper
TNFα	tumour necrosis factor alpha
WT	wild-type

Antibodies and Recombinant Cytokines/ Chemokines Used in ELISA detection

CYTOKINE/ CHEMOKINE	COATING ANTIBODY (WORKING CONC.)	STANDARD (PURIFIED CYTOKINE/ CHEMOKINE	CAPTURE ANTIBODY (WORKING CONC.)	ENZYME LABEL (WORKING CONC.)
Il-12p40	α-IL-12p40 mAb (#18491D) 1:1000	r-IL-12p40 (#19401W) (100ng/ml)	Biotinylated-α-IL-12p40/p70 mAb (#18482D) 1:1000	Streptavidin-alkaline Phosphatase (#13043E) (1:1000)
IFNγ	α-IFNγ mAb (#18111A) 1:500	r-IFNγ (#19301T) (100ng/ml)	Biotinylated-α-IFNγ mAb (#18112D) 1:1000	Streptavidin-alkaline Phosphatase (#13043E) (1:1000)
TNFα	α-TNFα mAb (#18131D) 1:1000	r-TNFα (#19321T) (100ng/ml)	Biotinylated-α-TNFα mAb (#18122D) 1:1000	Streptavidin-alkaline Phosphatase (#13043E) (1:1000)
MCP-1	α-MCP-1 mAb (#18241D) 1:500	r-MCP-1 (#19341V) (100ng/ml)	Biotinylated-α-MCP-1 mAb (#18272D) 1:1000	Streptavidin-alkaline Phosphatase (#13043E) (1:1000)

All antibodies utilised were purchased from Pharmingen.

Sensitivities:

IL-12p	100 pg/ml
IFNγ	15 pg/ml
TNFα	45 pg/ml
MCP-1	45 pg/ml

Reagents and Chemicals

Agarose	agarose gel (PCR)	Whitehead Scientific
Boric Acid	TBE buffer	Merck
Bromophenol blue	loading buffer	Merck
BSA fraction V	buffers	Sigma
Chloroform	DNA extraction	Sigma
Diethyl-ether	anaesthetic	Anala R
DNTPs	PCR reaction	Promega
EDTA	TBE buffer	Roth
Ethanol	DNA extraction	Anala R
Ethidium bromide	DNA staining	Fluka
Formaldehyde	tissue fixation	Merck
Gelatine	PCR buffer	Sigma
Glucose	PCR buffer	Anala R
Glycerol	*M.tb* culturing	Sigma
Heparin	anti-coagulant	Pharmacare-limited
Isopropanol	DNA extraction	Gibco
KCl	buffers	Merck
K_2HPO_4	buffers	Merck
LPS	endotoxin challenge	Sigma
Middlebrook 7H9	*M.tb* culturing	Difco
Middlebrook 7H10	Agar plates	Difco
$MgCl_2.6H_2O$	buffers	Anala R
NaCl	buffers	Merck
NaH_2PO_4	buffers	MERCK
OADC enrichment	*M.tb* culturing	State Vaccine Institute
p-Nitrophenylphosphate	ELISA	Boehringer Mannheim
Proteinase K	tail digestion	Sigma
Rapidiff Kit	differential counts	Clin. Sciences Diagnostics
SDS	lysis buffer	Pharmingen
Sodium azide	preservative	Merck
Taq enzyme	Super-Therm DNA polymerase	Biorad
Tris-base	TBE buffer	Sigma
Tris-HCl	lysis buffer	Sigma

Tris pH 9	PCR buffer	Sigma
Trypan blue	cell counting	Sigma
Tween20	washing buffer (ELISA)	Sigma
Tween80		
Xylene-cyanol	loading buffer	BHD chemicals